Energy & Buildings 265 (2022) 112085

Contents lists available at ScienceDirect

Energy & Buildings

journal homepage: www.elsevier.com/locate/enb

Experimental characterization of the coupling and heating performance of a CO_2 water-to-water heat pump and a water storage tank for domestic hot water production system

F.J.S. Velasco *, M.R. Haddouche, F. Illán-Gómez, J.R. García-Cascales

DITF, Universidad Politécnica de Cartagena, ETSII, Dr. Fleming s/n, 30202 Cartagena, Murcia, Spain

ARTICLE INFO

Article history:
Received 28 January 2022
Revised 20 March 2022
Accepted 3 April 2022
Available online 6 April 2022

Keywords:
Heat pump
Storage tank
Hot water production
CO_2

ABSTRACT

This work presents an experimental study of the dynamic performance of a CO_2 water-to-water heat pump in a domestic hot water production system. A facility was developed and used to characterize the time evolution of the COP of this heat pump, the heating and stratification processes of the hot-water storage tank, and the global COP of the system. Results showed that, when heating the water storage tank, strategies based on promoting stratification to reach Ri ∼40, such as the use of vertical tank filling velocities $v \sim 10^{-4}$ m·s^{-1} with low water flow rates between the tank and the heat pump gas cooler, permits an increase of ∼12.4% in the system global COP and a reduction of ∼16% of the compressor energy consumption compared to other strategies. However, strategies based on considering higher water flow rates (i.e. Ri ∼1) increase the thermal energy available in the tank (∼6% when flow rate and v increases a factor 3.6) but enhance the water mixing and extend the heating time which reduces the global COP of the system. Besides, an increase of the evaporator inlet water temperature from 5 °C to 20 °C increases the system global COP by 59% and reduces the heating time ∼40%.

1. Introduction

Ensuring a reliable, economical, and sustainable energy supply, as well as climate protection, are important global challenges of the 21st century. Some international agreements, such as the one committed by the European Union [1], propose to achieve between 80 and 90% reduction of greenhouse gas emissions by 2050 to reach climate neutral countries. The use of renewable energies and the improvement of energy efficiency are some of the most important steps to achieve these energy policy goals. Among others, the building sector is an important consumer where there is a key energy-saving potential. In fact, Heating, Ventilation and Air-Conditioning (HVAC) systems account for 40–60% of the energy consumption in buildings [2]. In Europe, hot water production represents around 15% of the total energy consumption in the household's sector [3]. Nowadays high efficient heat pumps can be considered a solution to replace fossil-fuel boilers, especially in the domestic hot water (DHW) production sector. This can be a key strategy to decarbonize existing buildings as well as to design carbon–neutral buildings and/or zero-emission buildings.

Among the different applications and technologies used in water-to-water heat pumps [4,5], groundwater or wastewater heat pumps raise as potential candidates for DHW generation and residential heating [6,7]. They use underground or in-house greywater lines as a thermal sink of the system, getting profit of the warmer temperature range of these lines compared to the outdoor ambient temperature to boost its coefficient of performance (COP). Besides, in the case of tertiary buildings, the hot water flow of the cooling towers can be also used in water-to-water heat pumps of hot water generation systems.

Many authors have focused their efforts on water-to-water heat pumps for hot water generation. Among them, Liangdong et al. [8] work stands out. They investigated experimentally the effect of the operating parameters on the heating performance of a cascade, wastewater, heat pump. Their results showed that the COP of the system decreases around 20% with the increase of tap water inlet temperature from 10 °C to 15 °C and about 11–13% with the increase of hot water outlet temperature from 40 °C to 50 °C. They also proved that increasing the flow rate of tap water and greywater can effectively improve the heating performance of the system. Another study interesting to highlight is that of Farzanehkhame-

Abbreviations: DHW, domestic hot water; Ri, Richardson number; COP, Coefficient of Performance.

* Corresponding author.
E-mail address: fjavier.sanchez@upct.es (F.J.S. Velasco).

https://doi.org/10.1016/j.enbuild.2022.112085
0378-7788/

Nomenclature

c_p	Specific heat ($kJ \cdot kg^{-1} \cdot K^{-1}$)
D	Inner diameter of the tank (m)
dh	Enthalpy (kJ)
du	Internal energy (kJ)
E	Energy (kJ)
g	Gravity ($m \cdot s^{-2}$)
H	Height (m)
$\dot{m}$	Mass flowrate ($kg \cdot s^{-1}$)
m, M	Mass (kg)
$\dot{Q}$	Thermal power (kW)
Ri	Richardson (−)
t	Time (s), (h)
T	Temperature (°C)
V	Volume (m^3)
v	Velocity ($m \cdot s^{-1}$)
$\dot{W}$	Electric power (kW)

Greek letters

β	Volume expansion coefficient (K^{-1})
Δ	Temperature difference (°C)
ρ	Density ($kg \cdot m^{-3}$)
τ	Dimensionless filling time (−)

Abbreviations

COP	Coefficient Of Performance
DHW	Domestic Hot Water
EEV	Electronic Expansion Valve
GC	Gas Cooler
GWP	Global Warming Potential
HP	Heat pump
HVAC	Heating, Ventilation and Air-Conditioning
IHX	Internal Heat Exchanger
ODP	Ozone Depletion Potential
PCM	Phase Changing Material
RMS	Root Mean Square
RTD	Resistance Temperature Detector

Subscripts

bottom	Bottom
cw	Cold water
evap	Evaporator
hw	Hot water
in	Inlet
top	Top

neh et al. [9] who made an energy economic assessment of the use of a geothermal heat pump as an air conditioning system for a residential building in a location with a cold semi-arid o steppe climate (BSk) and evaluated the potential reduction of the energy consumption. Their analysis showed that the payback period of the system was about 7.4 years with a low initial cost.

The use of CO_2 heat pumps for DHW production has a rising interest due to its sustainability and environmental potential, as it permits revaluing this substance in a future circular economy. In addition, the CO_2 (R744) is a natural refrigerant, non-toxic, non-flammable (i.e. type A1), and cheap. It has a 0 value of Ozone Depletion Potential (ODP) and a Global Warming Potential (GWP) of 1 [10]. For the building sector, low GWP type A1 refrigerants are postulated as highly recommended in future decarbonization policies in this sector. Currently, there are few low-GWP type A1 refrigerants able to compete with CO_2. In fact, heat pumps working with CO_2 are one of the most efficient heating generators for DHW using A1 refrigerants. Due to its low critical point (critical temperature of 31 °C), CO_2 is mainly used in heat pumps water heaters with *trans*-critical cycles. The use of these types of cycles allows CO_2 heat pumps to provide high COP values for heating water from very low inlet water temperatures as the heat transfer at the hot sink is performed with sensible energy (not latent energy) also at the refrigerant side of the heat exchanger, what increases its efficiency [11]. In contrast to subcritical cycles, in *trans*-critical cycles, the pressure at which the heat is transferred to the heat sink is not directly conditioned by the temperature of that sink. Thus, there exists an optimal operating pressure that depends on the specific working conditions of the heat pump [12,13]. Many authors have studied the optimal design and configurations to obtain high efficient CO_2 *trans*-critical heat pumps both experimentally and theoretically [4,14–16]. To assist in the design process of new models, it is a key issue not only to develop numerical models that permit the characterization of this type of hot water production system but also to provide ad-hoc experimental data to validate those models. Wang et al. [17,18] analysed numerically the performance of a CO_2 heat pump for a residential heating system using TRNSYS. The results presented for the system proposed therein show that the heating capacity and energy consumption of the proposed system decrease by 21% and 24%, respectively, in comparison with a baseline CO_2 transcritical simple compression system. Fernandez et al. [19] investigated the effect of the environmental conditions on the COP of a CO_2 heat pump water heater and they compared a two-stage cycle with an internal heat exchanger and a cycle with a suction line heat exchanger to a basic (i.e. baseline) cycle. They concluded that the overall COP increases when the ambient temperature increases, and by using a suction line heat exchanger they obtained an increase in the COP by up to 7.9 % compared to the baseline cycle under the same conditions. Kim et al. [20] investigated numerically and experimentally the influence of a heat exchanger on the performance of a *trans*-critical CO_2 cycle. They found that the geometrical parameters of the internal heat exchanger affect the mass flow rate of refrigerant. Moreover, they found that the compressor power consumption decreases with the increase of the length of the heat exchanger whereas the COP of the CO_2 cycle is improved. Yokoyama et al. [21] analysed numerically the influence of the hot water demand on the performance of a CO_2 heat pump. They concluded that the daily change in the hot water demand does not significantly affect the daily average system efficiencies. Hu et al. [22] studied experimentally an air-source *trans*-critical CO_2 heat pump water heater under different working conditions. Their results show that the higher hot water temperature can be reached by decreasing the inlet water flow rate or increasing the water inlet temperature. Among the different technologies available, vapour bypass cycles permit overcoming the traditional limitations found in basic cycles. Indeed, using the vapor bypassed upstream the evaporator has the potential for improving the performance of the system as it permits to decrease the refrigeranťs pressure drop of the evaporator of the heat pump. In general, and especially under high heating capacity conditions, the performance of a vapor bypass heat pump is always higher than that of a conventional one].

Besides the heat pump efficiency, other factors influence the energy efficiency of a hot water production system. The thermal

stratification of the hot water storage tank is one of these factors. Thermal stratification is usually employed in DHW storage tanks [23–25], and it is highly recommended for heat pumps water heaters to maintain a high energy performance. Gao et al. [25] studied experimentally and numerically different geometries of a central hole baffle plate to improve and characterize the thermal stratification of a DHW storage tank during the charging process. They performed an optimization process based on the Richardson number of the system as a representative descriptor of the stratification and provided a plate geometry and location as well as an inlet velocity that maximized the tank stratification. Wang et al. [26] experimentally investigated the effect of the inclusion of PCM balls on the thermal stratification of a hot water storage tank. They found that, for a fixed inlet flow rate, an improvement of the thermal stratification was achieved as the positions of the balls became closer to the inlet. Esen and Ayhan [27] developed a model of a cylindrical energy storage tank with PCM packaged in cylinders and the heat transfer fluid (HTF) flowing parallel to it. Their results show that some parameters must be investigated in order to optimize the thermal performance of the storage tank as the PCM properties, cylinder diameter, the mass flow rate, and the inlet temperature of the HTF. Chandra and Matuska [28] presented a numerical study using CFD of the stratification performance in DHW storage tanks. They analyzed the impact that three types of inlet devices (perforated inlet, slotted inlet, and simple inlet) had in the stratification process. They found that all devices performed similarly at low flow rate and high temperature difference between mean storage and water inlet (ΔT), whereas at high flow rate and low ΔT (typical conditions in heat pumps application) the slotted inlet performed better than the others.

Despite the abundance of works devoted to both, the study of heat pumps for DHW generation, and the study of the thermal stratification inside a hot water storage tank, there are very few works dedicated to the analysis of the overall performance of the system when a heat pump is coupled with a storage tank together in a DHW production system. Stene [29,30] studied a 6.5 kW CO_2 heat pump for combined space heating and hot water heating coupled with a cylindrical 200-liter DHW storage tank with a movable insulating plate. He performed several tests in hot water heating only mode, in which he studied the influence of several parameters (hot water temperature, evaporation temperature, or compressor discharge pressure). Due to the special characteristics of the storage tank that he used in his tests, hot and cold water never mixed inside the tank and, therefore the water inlet/outlet temperature at the gas cooler was kept constant during his tests and, in fact, water conditions inside the storage tank did not affect to the performance of the heat pump. Tosato et al. [31] also studied a 30 kW CO_2 heat pump for combined space heating, space cooling, and DHW generation, connected in series with two 750-liter storage tanks. During DHW generation tests, they reported an average COP of 5.0 during the first stage of the tank charging process, when the water temperature entering the gas cooler stayed between 10 °C and 14 °C, and an average COP of 4.1 for the total working period, that finished when water temperature entering the gas cooler reached 32 °C. They also performed a numerical study [32] in which they concluded that the higher COP during DHW generation was obtained for the highest water mass flow rate through the gas cooler. It must be taken into account that in their study, the water tank storage was not modeled, and the gas cooler inlet water temperature profile was taken from experimental data collected in [31]. Liu et al. [33] experimentally investigated the performance of a 3 kW CO_2 heat pump system coupled with hot and cold thermal storage. They studied the heating/charging process of the thermal storage tank analysing three parameters: compressor frequency (between 35 and 50 Hz), opening of the expansion valve (i.e. superheating degree) and the flow rates of hot and cold water loops in the evaporator and gas cooler. For their study, they used a 3 kW CO_2 heat pump with an initial temperature in both tanks of 27 °C. The tests run until the average temperature in the hot tank reached 60 °C. Therefore, Liu's tests were performed under transient conditions in both, evaporator and gas cooler. They concluded that higher compressor frequency (i.e. 50 Hz) provided better thermal stratification and a shorter heating time than a lower one. This also resulted in the better performance of the system. The opening grade of the expansion valve did not have a significant effect on the thermal stratification within the tank but, it affected the superheating degree at the evaporator outlet, influencing the evaporator temperature and this affected the heat pump performance. Sifnaios et al [34] developed a CFD numerical model for an 8.9 kW R600a heat pump connected to a 109.6-liter vertical cylindrical water tank that they validated using their own experimental data. They reported a maximum average COP of 3.23 during the charging process and, according to their conclusions, variations of water flow rates in the range from 0.12 to 0.24 kg·s-1 did not affect the performance of the system when diffuser plates are used both at the inlet and the outlet of the tank. Aguilar et al. [35] developed their own 1D numerical model to study the charge and discharge process in a compact 1.5 kW nominal heating capacity R134a DHW heat pump integrated in a 190-liter storage tank. In their case, the heat pump condenser coil was made of a 6 mm copper tube that looped 15 times and wrapped around the outside of the bottom of the tank. Therefore, the only water mass flow rate that affected the stratification inside the tank was the water mass flow rate during the tapping cycle. They studied three different tapping cycles (S, M, and L) according to Standard EN 16,147 [36] and found that the different stratification profiles obtained depending on the tapping cycle clearly affected the performance of the system. Li and Hrnjak [37] developed a study in a similar system. They studied a commercial residential R134a heat pump water heater whose condenser had two parallel tubes which were wrapped around a 250-liters (66 gallon) water tank. They simulated the system using a CFD commercial software and focused in the heating-up stage. According to their results, there is an upward flow layer confined in a very thin layer near the tank wall and the flow condition in this layer is critical to the interaction between the vapor compression system and the water tank. During heating-up, the flow filed in the tank would first change dramatically at the beginning and then stabilize.

Other key factors are the hydraulic design of the system and the management and control of the heating, charging, and discharging process of the hot water storage tank. All in all, these key issues define the overall performance of heat pumps as DHW production systems, and it is of utmost importance to assess the influence of these factors on the overall performance of the system. This assessment can be done based on international standards. Specifically, the EN 16,147 [36] is one of the international standards that allow to characterize the performance of these type of systems.

In the open literature, there are many works related to the performance of heat pumps for DHW generation or the filling or stratification of hot water storage tanks. However, there is a lack of studies that analyse the global dynamic performance of both units coupled together in a DHW production system. This work tries to contribute to the gap of knowledge. The objective of this work is to analyse the dynamic performance of DHW production system based on a CO_2 water-to-water heat pump during its operation under standard conditions (i.e. EN 16,147 conditions). Specifically, this work focuses on the evolution of the performance of the DHW production system, including the hot water storage tank, CO_2 heat pump and auxiliary elements, during the heating process of the hot water storage tank. For that purpose, a series of experimental tests have been conducted. The *trans*-critical CO_2 cycle proposed is controlled by electronic back-pressure and thermal expansion valves

and coupled with a high efficient IHX and a stratified water storage tank for improving the efficiency of the DHW generation system. An experimental facility was built and used to evaluate the energy efficiency of the system following the guidelines of the international standard EN 16147. The facility includes a hot water storage tank instrumented with temperature sensors to characterize the heat pump performance and the evolution of the stratification process. During the experimental campaign, the influence of the water flow rate control strategies of the CO_2 water-to-water heat pump on the overall efficiency of the system is analysed, paying attention to the influence of the water flow rate at the gas cooler and the evaporator as well as the inlet water temperature at the evaporator on the performance of the system. Besides, it is also an objective of the work to analyse the influence of the operation mode of the heat pump (i.e. transcritical or subcritical mode) on the performance of the DHW production system. The work is structured as follows: section 2 describes the test procedure followed for the characterization of the DHW generation system. In section 3 it is presented heat pump used and the overall DHW generation system considered in this study. It is also described here the experimental set-up developed, and the test matrix used to characterize the performance of the system. Then, in section 4, the results are analysed and discussed. Finally, in the last section, the most important conclusions are outlined.

2. Test methodology used for the characterization of the performance of the DHW production system

The test procedure used in this study for the characterization of the performance of a DHW generation system based on a CO_2 water-to-water heat pump is based on the EN 16147. Following this standard, the characterization process was structured in several temporal stages where the final condition of a stage is the initial condition of the following one. More specifically, the stages considered for the characterization of the water heating process during the test performed in this study were three:

- Stage A: Stabilization
- Stage B: Fill the accumulation tank and prepare the test set-up.
- Stage C: Determination of the water heating time.

Stages A and B correspond to test preparation. Stage A includes the time required for the instrumentation and the system to warm up. During stage B, the storage tank was filled with cold water at 10 °C. During this period, cold water must circulate in the accumulation tank until the outlet temperature is equal to the inlet temperature, within the allowed variation limit of ± 0.2 K. Stage C seeks to determine the time t_h necessary to heat the stored water from the initial condition (i.e. temperature of the cold water equal to 10 °C) to the first compressor stop caused by the tank thermostat (which is located at the top of the tank), when the tank temperature reaches 60 °C. This procedure follows the guidelines of the heating process of the EN 16,147 standard (stages A to C).

3. Description of the DHW production system and experimental facility

As previously said, the system developed in this work for DHW production consists of a CO_2 *trans*-critical water-to-water heat pump connected to a hot water storage tank which is fed by the domestic tap water network. Fig. 1a shows a layout of the heat pump developed in this study and the elements and instrumentation used. The heat pump consists of a semi-hermetic reciprocating compressor with a geometrical flow rate of 1.46 $m^3 \cdot h^{-1}$ at 50 Hz (i.e. $\sim$ 1.5 kW of electric power), three brazed plate heat exchangers working respectively as the evaporator, the gas cooler, and the IHX, a vessel for refrigerant storage, a back-pressure electronic valve (BPV) and an electronic expansion valve (EEV). The back-pressure valve controls the gas cooler pressure, whereas the expansion valve controls the superheat level at the evaporator outlet. The IHX permits reducing the quality of the refrigerant at the evaporator inlet. Table 1 enumerates the main components of the heat pump.

Fig. 1b shows two snapshots of the facility, one of the heat pump (left), and the other of the cold water storage tank used to prepare stage B and of the hot water storage tank (right). As shown in Fig. 1(a & b) the heat pump includes several valves and an IHX which allow the user to modify the operating cycle and test different configurations. In this work, the cycle without gas-bypass is considered (Fig. 1a). Regarding the instrumentation used for the characterization of the performance of the heat pump, it includes RTD temperature sensors, pressure sensors and flowmeters. Table 2 includes some of the specifications of the instrumentation.

Fig. 1c shows a schematic diagram of the hydraulic set-up of the experimental facility developed to afford the experimental characterization of the water heating process of the DHW production system following the procedure described in the previous section. The cold-water tank shown in the figure stores water at 10 °C and simulates the domestic tap water network. It permits feeding the hot water storage tank during DHW consumption process. The hot-water storage tank of the DHW production system is instrumented with RTD probes located in the cylinder axis to measure the water temperature at different heights. The tank is also equipped with valves, pumps, flowmeters, and temperature sensors to simulate the DHW consumption during the tests. This tank has a capacity of 0.772 m^3 and is connected to the gas cooler of the heat pump. The third tank is the water chiller tank, an auxiliary deposit that provides water to maintain the cold-water storage tank at 10 °C. Finally, the user tank collects the water extracted from the hot-water storage tank during the consumption process and distributes it to the system after the test.

The cold-water storage tank is controlled through a three-way valve and a PID controller and it is also connected to the water chiller tank to maintain it always at a specific temperature of 10 °C. The hot-water storage is one of the most important elements of this study, as its stratification is a key factor in the energy efficiency of the overall DHW production system. Thus, to characterize the stratification within the tank and the temperature transients during the consumption and filling processes, this cylindrical tank was equipped with 10Pt-100 RTD temperature sensors installed along its axis to analyse the behaviour of the water stratification. Note that the hot water storage tank is connected to the gas cooler of the CO_2 heat pump through ports A and C of Fig. 1a(right) which corresponds to ports LC1 and LC2 in Fig. 1c. The parameters of the hot water storage tank are illustrated in Table 3.

The test facility and the DHW production system are controlled through an in-house LabVIEW script whereas the data acquisition is performed via a high sampling frequency data acquisition system type cDAQ 9189 [38] and a low sampling frequency datalogger type Agilent 34970A [39] that scan the variables of the facility at the frequency required by each test. In these tests, data are sampled every 6 or 20 s.

3.1. Test matrix and characteristic variables of the test methodology

Table 4 shows the test matrix considered in this work. A total of nine tests were conducted to analyse the energetic performance of the DHW production system developed during the heating process. In all the cases the tests included an IHX. As previously indicated, the tests were designed following the procedure established at the EN 16,147 standard. The tests included different inlet and outlet

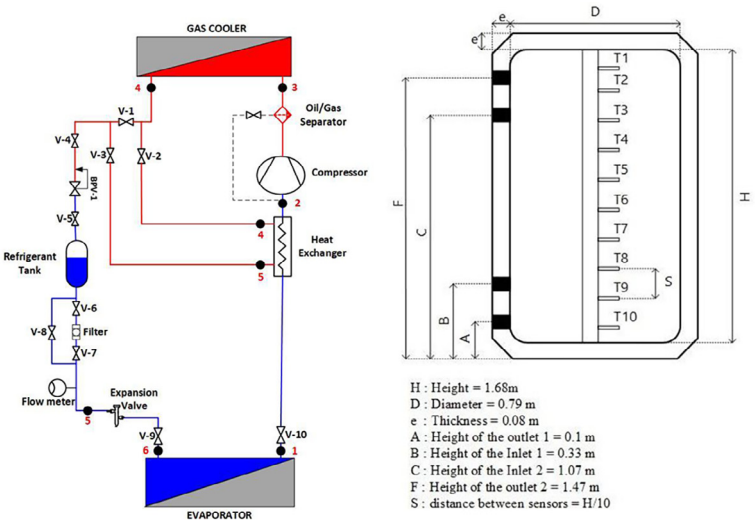

a)

b)

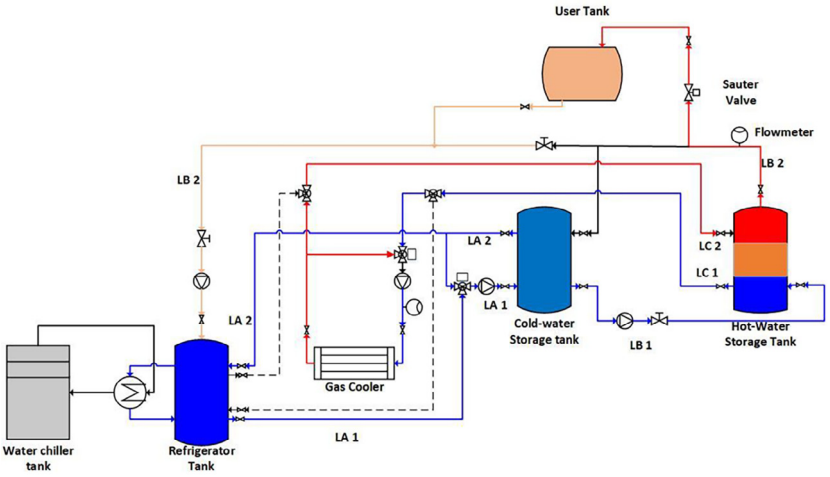

c)

Fig. 1. (a) Scheme of the heat pump (left) and hot water storage tank (right). (b) Snapshots of the experimental set-up: CO_2 water-to-water heat pump (left) and cold water and hot water storage tanks (right). (c) Schematic diagram of the hydraulic set-up of the experimental facility.

Table 1
Specifications of the components of the heat pump.

Elements	Manufacturer-Model
Compressor	DORIN CD300H
Evaporator	SWEP BX8T
Gas cooler	SWEP B16
IHXs	SWEP B17
Electronic expansion valve, back-pressure electronic valve	EV CAREL models E2V11CS100 and E2V24CS100

Table 3
Hot-water storage tank parameters.

Inner diameter of the tank (D)	0.79	(m)
Inner diameter of the ports (d)	0.034	(m)
Height (H)	1.68	(m)
Aspect ratio (H/D)	2.12	–
Insulation wall thickness	0.08	(m)
Insulation wall conductivity	0.025	($W \cdot m^{-1} \cdot K^{-1}$)
Insulation wall density	30	($kg \cdot m^{-3}$)
Insulation wall specific heat	1600	($J \cdot kg^{-1} \cdot K^{-1}$)

water temperatures and flow rates that were imposed and did not change with time. The inlet water temperature at the gas cooler was always 10 °C at the beginning of the test. There are two main parameters on which this study is focused: the flow rate in the gas cooler and the inlet temperature of the evaporator. The first five rows of the table are the tests where the evaporator conditions were constant, with an inlet and outlet temperature of 10 °C and 7 °C respectively, and the water flow rate at the gas cooler varied between 0.0833 $kg \cdot s^{-1}$ and 0.3 $kg \cdot s^{-1}$ with an increment of 0.055. Tests 6 to 9 were performed with a fixed gas cooler flow rate of ~ 0.3 $kg \cdot s^{-1}$ and a fixed evaporator flow rate of 0.544 $kg \cdot s^{-1}$. These tests were performed at the maximum gas cooler flow rate that can be reached in the facility (0.3055 $kg \cdot s^{-1}$). In this case, the inlet water temperature at the evaporator was imposed between 5 °C and 20 °C. Table 4 shows a summary of the test conditions considered in the evaporator.

During the tests, the heating tests (stage C), started operating and flowing water through the secondary side of the gas cooler to increase the tank water temperature from the initial value of 10 °C up to 60 °C. The tests finish when the temperature at the highest probe of the tank (i. e. T1) reached 60 °C. Based on the data recorded during the test, several characteristic variables were obtained. The global coefficient of performance of the DHW production system (global COP) was defined as the energy of hot water stored in the tank divided by the energy consumed by the compressor. It is worth noting that this definition of the global COP includes the information not only of the COP of the CO_2 heat pump but also of the efficiency in the final energy transfer to the hot water storage tank which is a function of the heating process and the tank insulation and aspect ratio. The energy of the recirculating pumps is neglected and thus:

$$globalCOP = \frac{E_{tank}}{E_{comp}} = \frac{\int_0^H \frac{\pi D^2}{4} \cdot \rho \cdot C_p \cdot (T_i(t = t_{tank}) - T_i(t = 0)) \cdot d\xi}{E_{comp}} = = \frac{\sum_{i=1}^{i=10} C_p \cdot (T_i(t = t_{tank}) - T_i(t = 0)) \cdot \Delta m}{E_{comp}} \quad (1)$$

where:

ρ is the water density in $kg \cdot m^{-3}$.

$T_i(t = t_{tank})$ -$T_i(t = 0)$ is the temperature variation of the measured water temperature at height level $i = i \cdot H/10$ of the tank during the heating period.

Δm: is one-tenth of the water mass of the tank (M) in kg (i.e. $M/10$).

C_p: is the specific heat of the hot water, in $kJ \cdot kg^{-1} \cdot K^{-1}$.

t_{tank}: is the heating time, i.e. the duration of the heating process to reach 60 °C at the top of the vessel in s.

E_{comp} is the electrical energy consumed by the compressor during a test in kJ.

Besides, the instantaneous COP of the system at any time during the heating period can be also obtained based on the formulae:

$$instantaneousCOP = \frac{dE_{tank}(t)}{dE_{comp}(t)} \quad (2)$$

where dE_{comp} is the electrical energy absorbed by the compressor during the time lapse dt in kJ and.

dE_{tank} (t) in kJ is obtained from:

$$dE_{tank}(t) = \int_0^H \frac{\pi D^2}{4} \cdot \rho \cdot C_p \cdot T_i(t) \cdot d\xi - \int_0^H \frac{\pi D^2}{4} \cdot \rho \cdot C_p \cdot T_i(t - dt) \cdot d\xi = = \sum_{i=1}^{i=10} C_p \cdot dT_i(t) \cdot \Delta m \quad (3)$$

And $dT_i(t) = T_i(t)$ -$T_i(t\text{-}dt)$ is the temperature variation of the measured water temperature at height level $i = i \cdot H/10$ of the tank during the heating lapse dt.

The instantaneous COP is obtained from Equation 2 at each time step of the data acquisition process during the test. Finally, an averaged or accumulated COP can be obtained for each time t of the heating process by considering the energy consumed by the compressor and the energy accumulated at the tank from the beginning of the test until instant t:

$$accumulatedCOP = \frac{E_{tank}(t)}{E_{comp(t)}} = \frac{\int_0^H \frac{\pi D^2}{4} \cdot \rho \cdot C_p \cdot (T_i(t) - T_i(t = 0)) \cdot d\xi}{E_{comp}(t)} = \frac{\sum_{i=1}^{i=10} C_p \cdot (T_i(t) - T_i(t = 0)) \cdot \Delta m}{E_{comp}(t)} \quad (4)$$

Table 2
Instrumentation characteristics and measurement uncertainty.

Sensor	Characteristics	Measurement accuracy	Range of measurement
Pressure sensors	Absolute sensor: Yokogawa EJX510A ECS // EJX510A ECS JDS	±2.1·kPa // ±5·kPa 0.04% and 0.05% of the measurement range.	0 – 5 MPa // 0 – 12 MPa
	Differential pressure sensor: Yokogawa EJX110A JHS	± 260 Pa. 0.26% of the measurement range	0 – 0.1 MPa
Temperature sensors	RTD Pt-100 class A 1/10 DIN	±0.1 K	223–523 K
Compressor electric power measurement sensor	Sineax M563	± 1% of the measured value in W	0 – 2.5 kW
Refrigerant flowmeter (mass flow rate at the refrigerant circuit)	Yokogawa RCCS32	± $5.28 \cdot 10^{-6}$ $kg \cdot s^{-1}$ ± 0.27% of the measured value in $kg \cdot s^{-1}$	0 – 0.1 $kg \cdot s^{-1}$
Water Flowmeter (flow rate at the water side of the gas cooler)	Siemens fm magflo mag1100 // Sitrans fm mag 5100w.	± $4.91 \cdot 10^{-7}$ $m^3 \cdot s^{-1}$ ± 0.2% of the measured value in $m^3 \cdot s^{-1}$	0 – $0.1111 \cdot 10^{-2}$ $m^3 \cdot s^{-1}$
Clock (time measurement)	Ni-DAQ system	0.001 s	–

Table 4
Test conditions considered at the evaporator in the study.

	Evaporator			Gas Cooler
Test N°	Water T inlet (°C)	Water T outlet (°C)	Water flow rate ($kg{\cdot}s^{-1}$)	Water flow rate ($kg{\cdot}s^{-1}$)
1	10	7	–	0.0833
2	10	7	–	0.1388
3	10	7	–	0.1944
4	10	7	–	0.25
5 (Reference Test)	10	7	–	0.3055
6	5	–	0.544	0.3055
7	10	–	0.544	0.3055
8	15	–	0.544	0.3055
9	20	–	0.544	0.3055

To characterize the heating process in a hot water storage tank with a water mass of M, a characteristic time t_c can be defined from the differential equation of energy conservation applied to the storage tank. Assuming that the water behaves as an incompressible fluid and that the pressure variations in this fluid during the experiments have negligible influence on its enthalpy, thus its internal specific energy and specific enthalpy can be expressed in terms of the water specific heat as $du = Cp{\cdot}dT$ and $dh = Cp{\cdot}dT$. In this case, it is also considered that Cp variations within the temperature range of the experiments have a negligible impact on the results. Neglecting the kinetic and potential energy terms and viscous and radiative process, the energy conservation equation for the hot water storage tank could be expressed as:

$$M \cdot Cp \frac{d}{dt} \underset{\text{Tank Volume}}{\iiint} T(x,t)dV = = \underset{\text{Tank wall}}{\iint} h(T_w - T(x_{wall},t))dS_w + \dot{m} \cdot Cp \cdot (T_{hw}(t) - T_{cw}(t)) \quad (5)$$

where V is the tank volume, T is the local temperature of the water at any point "x" within the tank, h and S_w are respectively the convective wall heat transfer coefficient and the surface of the walls of the tank, $T_{hw} - T_{cw}$, in K, is the temperature difference of the hot water and the cold water at the inlet and the outlet of gas cooler (which are connected to ports A and C of Fig. 1a(right)) and $\dot{m}$ is the water flow rate at the gas-cooler in $kg{\cdot}s^{-1}$. Note that in Equation 5 uniform conditions have been considered at the inlet and outlet of the storage tank. Since the first right-hand side term is usually, two orders of magnitude smaller than the second one, the characteristic time of the process can be defined as:

$$t_c = \frac{M}{\dot{m}} \quad (6)$$

this characteristic filling time expresses the time needed by the hot water to flow through a tank of height H, and reach its bottom taking into account the characteristic vertical velocity of the flow within the tank which is of the order of $\sim 4\dot{m}/\left(\rho\pi D^2\right)$ and the dimensionless filling time is:

$$\tau_{filling} = \frac{4\dot{m}t_{\tan k}}{H\rho\pi D^2} \quad (7)$$

Besides, the dimensionless heating time can be defined based on the nominal power of the heat pump used in the system and the tank capacity. This dimensionless number permits to estimate and compare the efficiency of the DHW production system with other units of different power and/or hot water tank capacity and depends on the heat pump/tank coupling:

$$\tau_{heating\ HPTank} = \frac{t_{tank}}{\frac{M \cdot C_p \cdot (T_{hwr} - T_{cwr})}{\dot{Q}}} = \frac{t_{tank}}{M \cdot C_p \cdot (T_{hwr} - T_{cwr})} \dot{W} \cdot \mathrm{COP_{ref}} \quad (8)$$

where the heating power transferred at the gas cooler of the CO_2 heat pump is:

$$\dot{Q} = \dot{m} \cdot C_p \cdot (T_{hw} - T_{cw}) \quad (9)$$

In these equations $\dot{Q}$ is the nominal thermal power of the heat pump, $\dot{W}$ is the nominal electric power of the heat pump compressor (1.7 kW in our case), $\mathrm{COP_{ref}}$ is a reference averaged value of the COP of the heat pump used. In this case, a value of $\mathrm{COP_{ref}} = 1$ was adopted in the non-dimensionalization to have a clear basis of comparison with other heat generators (for example, based on Joule effect) and/or with other heat pumps based on the nominal compressor power. Note that this dimensionless parameter could be also defined in terms of a nominal reference COP value (for example $\mathrm{COP_{ref}} = 3$), or any other nominal performance value of the associated heat pump, to reach values of $\tau_{heatingHPTank} \sim 1$ in the design process of a domestic hot water production system. T_{hwr} *and* T_{cwr} are the reference temperatures, in this case, 60 °C and 10 °C respectively.

Regarding the operation mode of the CO_2 heat pump, during the tests it was identified the working cycle of the heat pump by recording the working pressure of the refrigerant at the gas cooler and comparing it with the critical pressure of the CO_2 in order to assess whether the heat pump was working with a subcritical or a transcritical cycle. After this identification of the working cycle was performed online and link to the time during heating process of the hot water storage tank, this way the potential impact of the operation mode on the COP of the DHW production system was analysed.

The uncertainty analysis of the experimental results was performed following the ISO standard [40]. Based on the accuracy of the different sensors and data acquisition systems specified by the manufacturers the "type B uncertainty" of each measured quantity was estimated. Besides, the uncertainty of type A has been calculated based on the standard deviation of the recorded data with respect to the local average value of the variable considered. Error propagation procedure was used to estimate the combined standard uncertainty of the final quantities considered in the study as a function of the measured ones. A confidence level of 95% (i.e. k = 2) was used to express the expanded uncertainty of the parameters of interest. Table 5 shows the absolute and relative experimental uncertainty obtained:

4. Results and discussion

In this section, the experimental results are used to assess the influence of different factors on the performance and efficiency of the DHW production system. First, the results of the experimental tests are described. Later the influence of different key parameters and strategies on the performance of the DHW production system are discussed.

4.1. Experimental tests

Fig. 2a shows the evolution of the temperature of the hot water storage tank with time during the heating process (stage C) for the

Table 5
Experimental uncertainties obtained in the final quantities during the experiments.

Quantity	Absolute Uncertainty	Range measured	Relative uncertainty measured (%)	Maximum Uncertainty accepted by EN 1647
Temperature (K)	±0.1	273–473	± 0.04 – 0.02	±0.2
Water flow rate ($m^3 \cdot s^{-1}$)	$\pm 0.00153 \cdot 10^{-3}$	$0.0830 - 0.306 \cdot 10^{-3}$	± 0.5	±1 %
Compressor power (kW)	±0.011 – 0.017	1.1 – 1.7	± 1 %	±1 %
E_{comp} (kJ)	±0.066 – 0.149	39600–63700	less than0.0004 %	±1 %
E_{tank} (kJ)	±0.156 – 0.255	147500–195300	less than0.0002 %	±5 %
Global COP	± 0.022 – 0.035	2.49 – 3.97	± 0.87 %	–

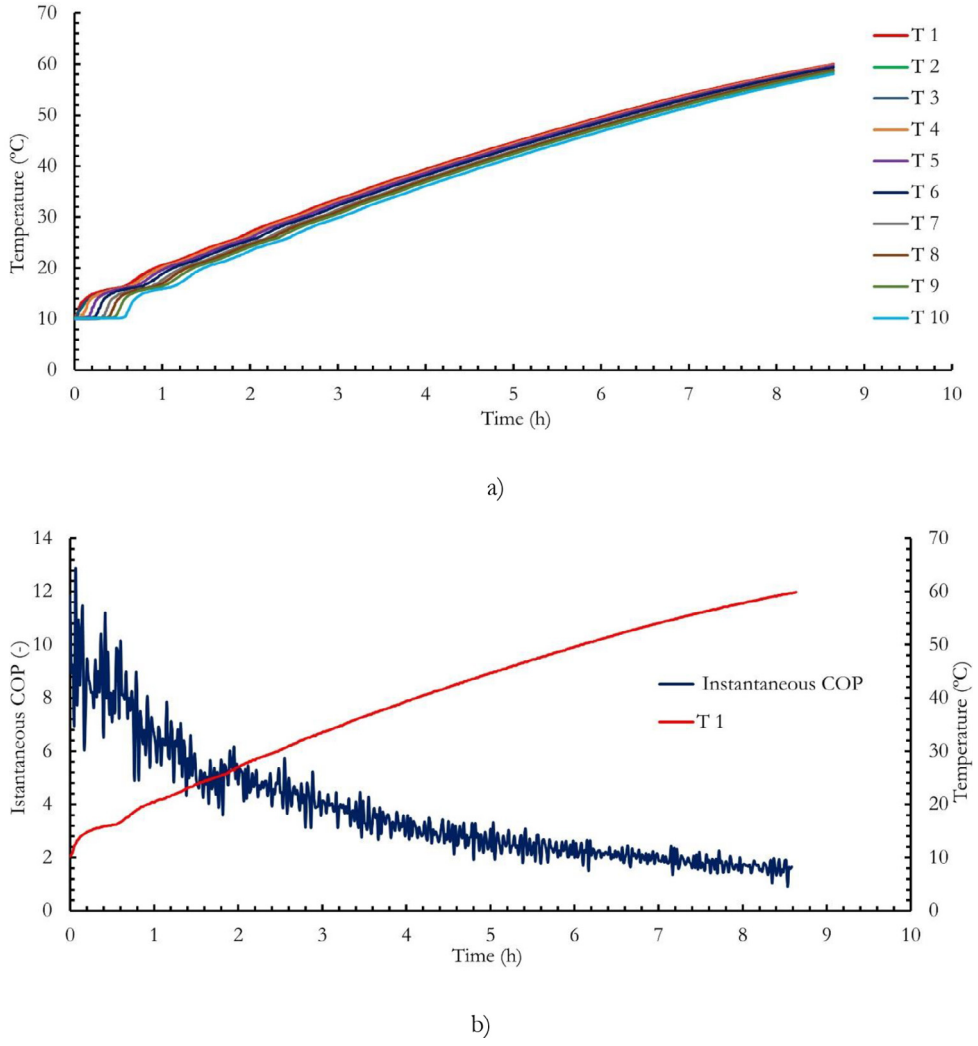

Fig. 2. (a) Evolution of the tank temperature for the 10 probes inside the tank for test number 5. (b) Evolution of the instantaneous COP of the DHW production system with time and evolution of water temperature at the top of the storage tank (T_1) for test 5.

temperature probes located at different heights within the tank for test number 5 (reference test) where the heat pump heats up the water of the storage tank (0.772 m^3) from 10 °C to 60 °C with a gas cooler flow rate of 0.305 $kg \cdot s^{-1}$. As shown, temperature evolution during the initial period of the heating process shows fluctuations that are related to the heating capacity of the heat pump ($\dot{Q}$), but also to the storage tank mass (M). These parameters define the water injection temperature as well as the filling and heating characteristic times. For the conditions of this test, after the first third of the total heating period pass by, the temperature evolution at different heights become self-similar, monotonically increasing curves that slightly tend to converge due to thermal diffusion. This transport phenomenon reduces the temperature gradient between the top and the bottom of the storage tank and promotes this convergence. Fig. 2b shows the dynamic evolution of the tank temperature and the instantaneous COP of the DHW production system as a function of time during the heating process (stage C). As shown, in this test the heating process last for 8 h and 38 min and has a characteristic time of t_c = 2527 s which corresponds to a dimensionless filling time of $\tau_{filling}$ = 12.3 and a dimensionless heating time of $\tau_{heatingHPTank}$ = 0.328 which shows that the heating process requires ~ 12 times the characteristic time need by the water flow

to traverse the tank height and around ~ 1/3 of the time needed to heat up the tank to the target T_{hwr} by Joule effect. As previously said, the global coefficient of performance of the DHW production system (global COP) is defined as the energy of hot water stored in the tank divided by the energy consumed by the compressor. At the beginning of the process, the instantaneous COP of the system is very high, however, as the temperature of the water in the tank increases, the instantaneous COP of the DHW production system decreases asymptotically. This is due to the performance provided by the CO_2 heat pump (i.e. COP of the heat pump) that shows a similar tendency with time to the one shown by the instantaneous COP of the DHW production system in Fig. 2b. This decreasing tendency with time is due to the fact that a CO_2 heat pump has higher efficiencies for low water inlet temperatures [11]. Since the gas cooler works in counter-flow condition, as the temperature of the water at the bottom of the hot storage tank increases, it also increases the refrigerant temperature at the gas cooler exit and the optimal pressure of the CO_2 cycle. Consequently, the heat pump control system acts increasing the gas cooler pressure seeking to reduce the refrigerant quality at the inlet of the evaporator which also increases the compression work. In other words, as the water at the inlet of the gas cooler increases, the quality of the refrigerant at the exit of the expansion valve as well as the compression work (Fig. 1a) increase reducing the specific heat absorbed at the evaporator and reducing the COP of the heat pump. This increase in the quality of the refrigerant and COP reduction would be higher in the case of a control strategy based on a constant gas cooler pressure. As a result, as the temperature of the water at the bottom of the tank increases during the heating process the COP of the heat pump decreases and the instantaneous COP of the DHW production system decreases with time.

Table 6 shows a summary of the tests results of the experimental campaign (Table 4). The first columns show the time-averaged global COP during the heating period (stage C) and the root mean square (RMS) of the instantaneous COP. It is worth noting that, as the instantaneous COP is a dynamic variable that changes with time, its RMS value was computed based on the dispersion of the sampled data with respect to the moving average of the instantaneous COP with 9 samples (i.e. the time-average of 180 s):

$$RMSinstantaneousCOP = \sqrt{\frac{\sum_{i}^{n}\left(x_i - \bar{x}_i\right)^2}{n^2}} \tag{10}$$

where n is the number of samples taken, x_i is the sampled value of the instantaneous COP and $\bar{x}_i$ is the moving average of the instantaneous COP:

$$\bar{x}_i = \frac{\sum_{j=i-4}^{i+4} x_j}{9} \tag{11}$$

As shown, both the heating time and the global COP of the DHW production system vary with the water flow conditions at both the evaporator and the gas cooler. The CO_2 heat pump COP and the instantaneous COP of the DHW production system show similar dynamic tendencies with time and with the key variables. The difference between both COPs values is due to the losses during the heating process. This difference is of the order of ~0.35. As time pass by, the water at the bottom of the tank heats up and the heat pump COP and the global COP of the DHW production system decreases with time. In general terms, the average of the instantaneous COP at the last third of the heating period is between 2 or 3 times lower than in the first third of the heating period. For fixed evaporator conditions, heating time (t_{tank}), accumulated energy (E_{tank}), the thermal power transferred by the heat pump to the water (named as "gas cooler thermal power" in Table 6), and global COP depend on the water mass flow rate through the gas cooler. As can be deduced from the values provided in Table 6 for test number 1 to test number 5, this dependency produces a maximum variation of around 13.6 % in the case of t_{tank}, 6.1 % in the case of E_{tank}, 9.7 % in the case of gas cooler thermal power and 12.8 % in the case of global COP. The following subsections discuss the results obtained in detail.

4.2. Impact of the gas cooler water flow rate

In tests 1 to 5, the influence of the gas cooler flow rate on the performance of the system is analysed by imposing constant conditions in the evaporator and varying the gas cooler flow rate. These five tests were conducted by varying the flow rate in the gas cooler from 0.0833 kg·s^{-1} to 3.055 kg·s^{-1} with an increment of 0.055 kg·s^{-1} between tests. Fig. 3a shows the temperature evolution of the water storage at the bottom of the tank (probe T_{10}) for the different tests. As shown, the temperature fluctuations shown in Fig. 2a are also shown here for different mass flow rates. In the case of Fig. 3a the temperature oscillations change with the flow rate which indicates that these fluctuations are a function of T_{hw} and v, the injection velocity of the hot water within the storage tank, which are magnitudes changed during these tests. Since the averaged thermal power transferred by the heat pump in the gas cooler does not vary significantly between tests (less than 10%), the reduction of the gas cooler flow rate to one-third results in a reduction of the characteristic vertical velocity at the storage tank $v \sim \frac{4\dot{m}}{\rho\pi D^2}$ of the same order and an increase of T_{hw}. Both tendencies

Table 6
Results of the experimental tests.

Test number	1	2	3	4	5	6	7	8	9
Global COP	3.688	3.487	3.386	3.269	3.280	2.489	3.286	3.867	3.967
RMS instantaneous COP	0.023	0.023	0.024	0.032	0.029	0.019	0.186	0.039	0.057
Heating time t_{tank} (ks)	27.70	29.34	30.35	31.48	31.13	42.75	31.28	26.57	25.93
t_c (s)	9268	5562	3971	3088	2527	2527	2527	2527	2527
$\tau_{filling}$	2.99	5.27	7.64	10.19	12.32	16.92	12.38	10.51	10.26
$\tau_{heating\ HP\text{-}Tank}$	0.29	0.31	0.32	0.33	0.33	0.45	0.33	0.28	0.27
Average of the instantaneous COP in the 1st 1/3 of the heating period	5.818	5.990	5.711	6.119	6.215	3.991	6.059	7.304	7.695
Average of the instantaneous COP in the last 1/3 of the heating period	2.442	2.190	2.085	1.945	1.942	1.659	1.756	2.238	2.318
Gas cooler thermal power (kW)	5.617	5.528	5.600	5.120	5.365	4.566	5.470	5.976	5.696
Compressor Power (kW)	1.385	1.447	1.491	1.406	1.516	1.420	1.534	1.486	1.385
E_{tank} (MJ)	149.1	153.1	154.9	157.5	158.2	158.5	158.1	157.6	157.5
E_{comp} (MJ)	40.42	43.91	45.73	48.17	48.24	63.67	48.12	40.75	39.70
Outlet gas cooler Temperature (K)	299	293	290	288	287	287	287	288	288
Tank vertical velocity $\frac{4\dot{m}}{\rho\pi D^2}$ (mm·s^{-1})	0.172	0.286	0.401	0.515	0.630	0.630	0.630	0.630	0.630
Time-averaged COP of the CO_2 heat pump	4.021	3.953	3.944	3.733	3.756	3.155	3.813	4.272	4.249

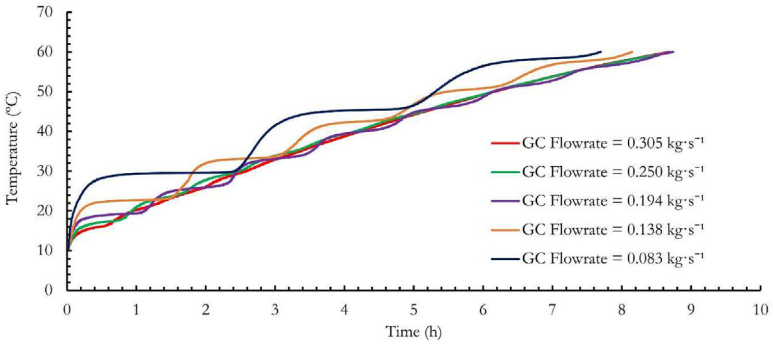

a)

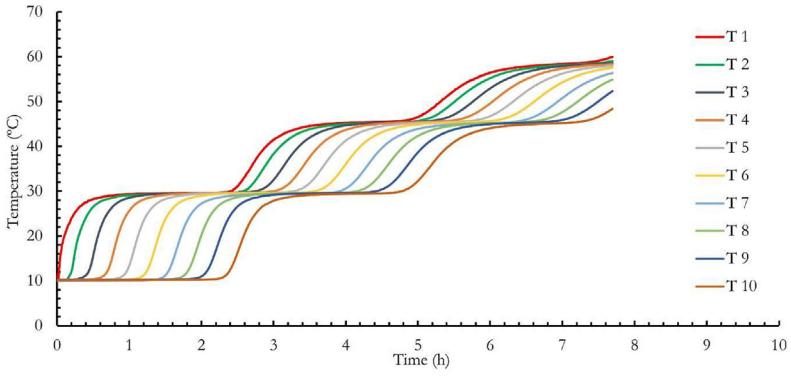

b)

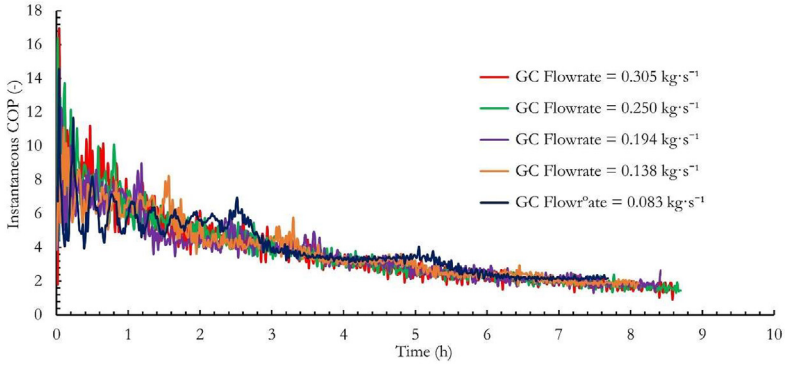

c)

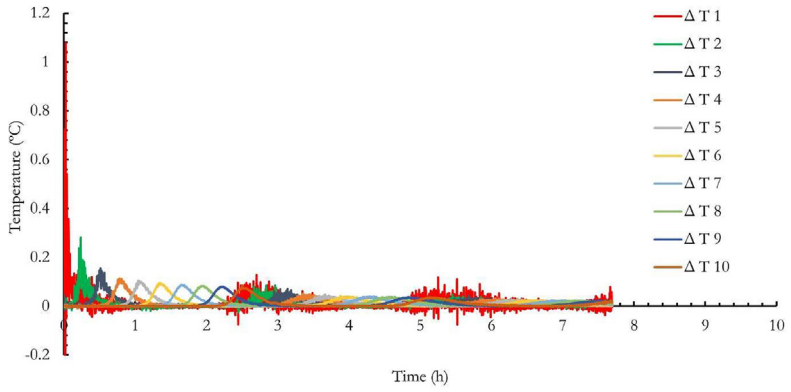

d)

Fig. 3. (a) Temperature T_{10} evolution with time for different water flow rates at the gas cooler. (b) Temperature evolution at different heights of the storage tank for low gas cooler flow rate (0.083 kg·s^{-1}). (c) Instantaneous COP evolution with time for different gas cooler flow rate. (d) Evolution with time of the dT_i at different hot water storage tank heights for the case of 0.083 kg·s^{-1}.

tend to promote water stratification within the tank. As a consequence, as the hot water mass flow rate decreases the amplitude and period of the oscillations measured increases due to the enhancement of the stratification process promoted by the T_{hw} and v tendencies of variation. This is somehow expected as the stratification tends to inhibit the water mixing and reduces the intensity of the turbulence mechanism and other transport phenomena that slow down the convective heat transfer. As a result, the thermal inertia of the mass water at the tank increases and the rate of change of water temperature with time decreases.

Fig. 3b helps to clarify these ideas. The figure shows the temperature evolution with time at different heights of the hot water storage tank during the heating process for test 1 (the lowest water flow rate at the gas cooler). As shown, the temperature at different heights shows self-similar profiles. The lower water layer at the bottom of the tank (T_{10}) shows a delay in the heating process with respect to T_1 at the top of the tank of the order of $\sim t_c$ which is due to the time required by the hot water to travel through the water tank height at the vertical characteristic velocity $v \sim \frac{4\dot{m}}{\rho\pi D^2}$. Besides, this figure shows that for this test (test 1) the heating process does not follow a continuous increasing tendency as in test 5 (Fig. 2a). On the contrary, in this case, the temperature profiles exhibit several "steps" which are related to the heating capacity of the heat pump used in the DHW production system. These temperature steps are of the order of $\sim \frac{\dot{Q}}{\dot{m}\cdot C_p} = \frac{\dot{W}\cdot COP}{\dot{m}\cdot C_p}$. In the first 9200 s, the heat pump is only able to heat up the water within the gas cooler from 10 °C to 22 °C. However, when the temperature of the water at the inlet of the gas cooler (T_{10}) starts increasing, also the temperature at the exit of the gas cooler (T_1) starts increasing. The height of these "steps" reduces as the water at the bottom of the tank increases (T_{10}) because the COP of the heat pump reduces with the increase of the inlet temperature at the gas cooler (Table 6). Moreover, the use of a small gas cooler flow rate in test 1, provides low thermal energy to the hot water storage tank that needs more "steps" to reach the reference T_{hwr} (60 °C in this case), than in the case of high gas cooler gas flow rate. Note that, in general terms, as the ratio of heat pump heating capacity to the tank mass increased, the number of "steps" would reduce. This clearly shows that when the heating power of a heat pump is limited with respect to the capacity of a hot water storage tank is of major importance to correctly choose the water flow control strategy. In other words, relatively "small" heat pumps coupled with relatively "big" water storage tanks will exhibit different performances and efficiency rates depending on the water flow rate at the gas cooler.

The evolution of the instantaneous COP as a function of time is shown in Fig. 3c. As shown, the instantaneous COP of the system decreases as time evolves and with the increase of the gas cooler flow rate. In the case of lower flow rates, the thermal stratification is formed and maintained (Fig. 3b), and this has an important benefit for the thermodynamic performance of the heat pump and the global COP of the DHW production system (Fig. 3c). However, as the gas cooler flow rate increases, the thermal stratification decreases and the water temperature in the storage tank becomes more homogenous, requiring more working time of the heat pump to reach T_{hwr} temperature at the top of the tank. As a result, more energy is accumulated in the tank.

Finally, Fig. 3d shows, the instantaneous variation of the water temperature with time ($dT_i = T_i(t) - T_i(t-dt)$ where t is the time of the measurement and dt is the sampling time of the data logger) at different heights of the hot water storage tank during the heating period for the case of low mass flow rate (0.083 kg·s^{-1}). As shown, the mass of water in a stratified tank exhibits different temperature heating "jumps" depending on the height within the tank where the temperature is measured. The lower layers of stratified water at the bottom of the tank notice lower heating jumps in a wider time-lapse than the layers of stratified water at the top of the tank where the heating jumps are sharper in time and more intense in temperature jump. This is due to the diffusion and transport phenomena taking place within the tank that tend to dump these jumps. Note that each temperature sensor measures two temperature heating "jumps" that are related to the regions of maximum temperature slope in Fig. 3b. For example, sensor T_1 notice a jump at the beginning of the heating period and another after a time of the order of $\sim t_c$. Thus, the temperature heating "jumps" found in Fig. 3d are related to the moments of the tank heating where a water layer feels the higher heat transfer due to the higher temperature lift at the gas cooler which are the moments when the temperature at the top and the bottom of the tank are similar and/or closer. Thus, the characteristic travel velocity of these heating waves along the tank (from top to bottom) is $v \sim \frac{4\dot{m}}{\rho\pi D^2}$. It is worth noting that these fluctuations in the water temperature at the tank influence very little in the COP of the CO_2 heat pump as the water entering the gas cooler is obtained from port at the bottom of the stratified tank (T_{10}) and the temperature variations with time of this tank region are the lowest ones. Table 7 and Fig. 4 show quantitatively the influence of the gas cooler flow rate on the global COP of the DHW production system and on the time-averaged COP of the CO_2 heat pump. The time-averaged COP of the CO_2 heat pump is defined as: $COP_{\text{Time averaged}} = \frac{\int_{t=0}^{t=t_{tank}} \dot{Q}dt}{\int_{t=0}^{t_{tank}} \dot{W}dt}$ where t_{tank} is the elapsed time during each test. It can be seen that the global COP decreases with the increase of the gas cooler flow rate. The highest performance value is given by the lower flow rate of the gas cooler. Again, this is due to the lower inlet temperature of the gas cooler caused by the thermal stratification that enhances the heat pump COP. As previously noticed, the gas cooler mass flow rate also has an influence on the energy storage in the tank. In fact, a reduction in the gas cooler mass flow rate of $\sim$ 72% results in a reduction of $\sim$ 6% in the overall thermal energy stored in the tank which means a $dE_{tank}/d\dot{m} \approx 41$ (kJ·s·kg-1).

4.3. Impact of the evaporator inlet temperature

To analyse the impact of the inlet temperature of the evaporator ($T_{in\ evap}$), tests 6 to 9 were performed by varying the inlet temperature in the evaporator between 5 °C and 20 °C. Results show that, as $T_{in\ evap}$ increases, the global COP of the system increases. Table 6 shows a variation of 59% in the global COP of the DHW production system between an inlet evaporator temperature of 5 °C and 20 °C. Fig. 5a shows the evolution of the storage tank temperature as a function of time for different tests. Two effects can be seen, on the one hand, temperature increases with time and, on the other, the heating time decreases as the evaporator inlet temperature increases, which is due to the refrigerant temperature difference between the inlet and the outlet of the evaporator. Also, it is noticeable that the heating time is greater as the water inlet temperature at the evaporator increases. For example, the heating time

Table 7
Influence of the gas cooler flow rate on the global COP of the DHW system and the time-averaged COP of the CO_2 heap pump.

Gas cooler flow rate kg·s^{-1}	Global COP of the DHW production system	Time-averaged COP of the CO_2 heat pump	Thermal energy storage E_{tank} (kJ)
0.083	3.688	4.021	149.1
0.138	3.486	3.953	153.1
0.194	3.386	3.944	154.9
0.25	3.269	3.733	157.5
0.305	3.280	3.756	158.2

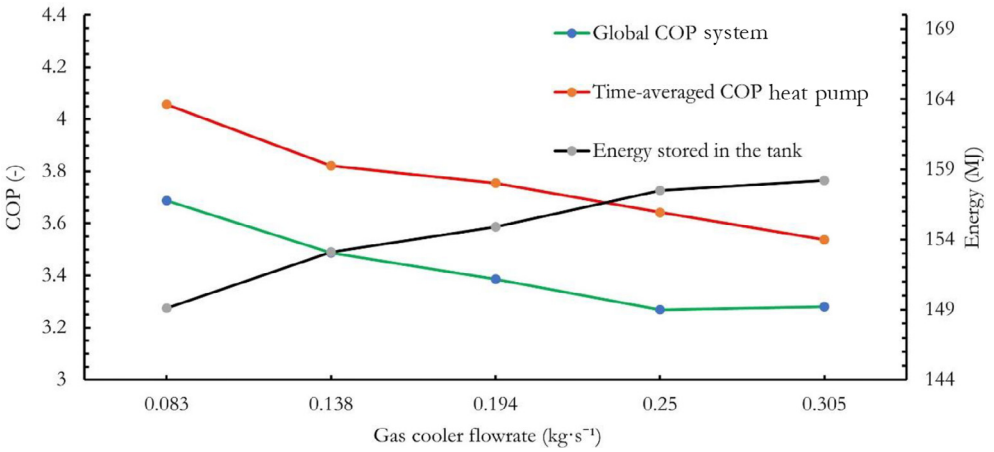

Fig. 4. Evolution of the Global COP of the DHW production system and time-averaged COP of the CO_2 heat pump with gas cooler mass flow rate.

is about 12 h when the water inlet temperature in the evaporator is 5 °C and is about 7 h for the case of an evaporator inlet temperature of 20 °C. This means a total reduction of ~ 40% and reduction of the heating time of 2.7% per degree increased at the inlet evaporator water temperature (i.e. $dt_{tank}/dT_{in\ evap} \sim 1/3$ (h/ °C)).

The heat pump performance is presented in Fig. 5b. This figure shows the evolution of the instantaneous COP of the system as a function of time. It can be seen that the instantaneous COP decreases with the increase of time, and this is due to the increase of the inlet temperature to the gas cooler, hence, when the storage tank temperature increases, the inlet temperature in the gas cooler increase. Also, the evaporator temperature influences in a negative manner the system performance, so, when the inlet temperature is higher, the system gives higher COP. Fig. 5c shows the evolution of the accumulated COP of the system as a function of the heating time for different water inlet temperatures at the evaporator. As shown, the accumulated COP shows the same decreasing evolution with time as the instantaneous COP, but in this case, the trends are clearer than in the previous case as this variable does not account for the high-frequency fluctuations of the instantaneous COP which are linked to the slight temperature oscillations between each sample during data acquisition. As shown, in the first hour of the heating period, the inlet water temperature at the evaporator has an important impact on the COP of the system. As the evaporator inlet temperature ($T_{evap,in}$) increases, the accumulated COP also increases gradually, from an initial value of 7 for $T_{evap,in}$ = 5 °C, to 9 for $T_{evap,in}$ = 10 °C, 10.5 for $T_{evap,in}$ = 15 °C, up to 12 for $T_{evap,in}$ = 20 °C. After the first hour the accumulated COP values tend to slowly converge.

4.4. Discussion on the stratification and the control strategy of the DHW production system

In order to analyse the thermal stratification within the hot water storage tank, two tests are taken into consideration under the same conditions but with the lower and the higher water mass flow rate at the gas cooler (test 1 and test 5). Fig. 6a shows the evolution of the tank temperature at different heights for both tests as a function of time. As shown, the temperature of the storage tank under the low flow rate conditions results in a slower heating process of the different water layers within the tank. These layers maintain a thermal stratification within the storage tank. As a result, the hot water injected from the gas cooler remains at the upper layer of the tank (T_1) and this layer reaches the target temperature T_{hwr} faster than in the case of test 5, which results in a shorter global heating time. In contrast, the heating time to reach T_{hwr} at the top of the tank with the higher flow rate last more time and the vertical temperature gradient within the tank is smaller during the heating process.

To characterize this stratification, Fig. 6b shows the time-averaged Richardson number during the heating process for different gas cooler mas flow rates and Fig. 6c shows the Ri evolution with time defined as $Ri = g{\cdot}\beta{\cdot}H'{\cdot}(T_1\text{-}T_{10})/v_{in}^2$ during the heating process for different mass flow rates. Ri number describes the ratio of the buoyancy to the mixing force and is a usual descriptor of the stratification. A large Ri indicates a stratified storage tank whereas a small Ri means a mixed storage tank. Note that, we follow the definition of Richardson number of [41,42] where H' represents the vertical distance between the inlet an outlet water ports of the tank, v_{in} is the inlet velocity of the water to the tank. The time-averaged Ri is computed following the mean value theorem as:

$$time-averaged\ Ri = \frac{1}{t_{tank}} \int_{t=0}^{t=t_{tank}} Ri^* \cdot dt \tag{12}$$

where Ri* is the instantaneous value of the Richardson number at the instant "t" of time. As shown in the figures, the time-averaged Ri for the lowest mass flow rate (0.083 kg·s^{-1}) is ~ 50 whereas for the case of the highest mass flow rate (0.305 kg·s^{-1}) is below 1. In other words, a reduction of a factor of 3.7 in the mass flow rate results in an increase of the stratification in a factor of 50. In fact, in this case, the Ri scales with the inverse of the power of the gas cooler mass flow rate following a potential law: $Ri = 0.00174/\dot{m}^{3.2}$ (with a fitting R^2 = 0.9993). Indeed, due to the heat pump-storage tank coupling, the Ri number can be written as a function of the COP of the CO_2 heat pump as:

$$Ri = \frac{g\beta H'(T_{top} - T_{bottom})}{v_{in}^2} = \quad = \frac{g\beta H'(T_{top} - T_{bottom})}{\left(\frac{4\dot{m}}{\rho\pi d^2}\right)^2}$$

$$\approx \frac{\pi^2 d^4 g \cdot H' \cdot \rho^2 \cdot \beta \cdot \dot{W} \cdot COP}{16 C_p \cdot \dot{m}^3} \tag{13}$$

This way, the stratification reached at the hot water storage tank can be linked with the design and operational parameters of the CO_2 heat pump and its efficiency. Note that, this approximation of the Ri as a function of the COP of the heat pump is valid for the case of negligible thermal losses (i.e. temperature losses ΔT_{losses}) in the pipes connecting the heat pump and the hot water storage tank

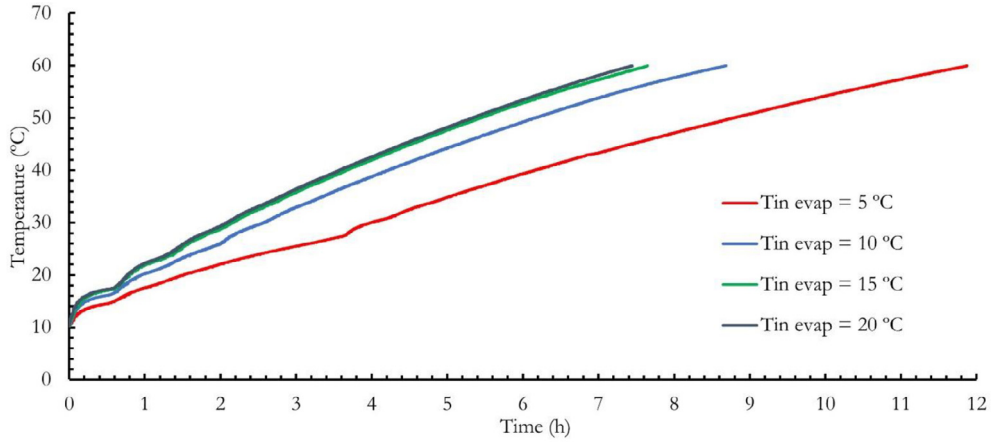

a)

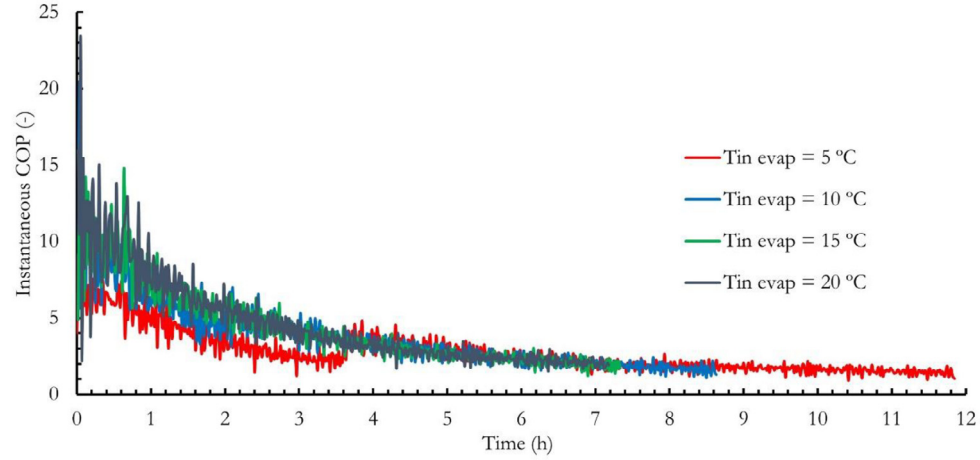

b)

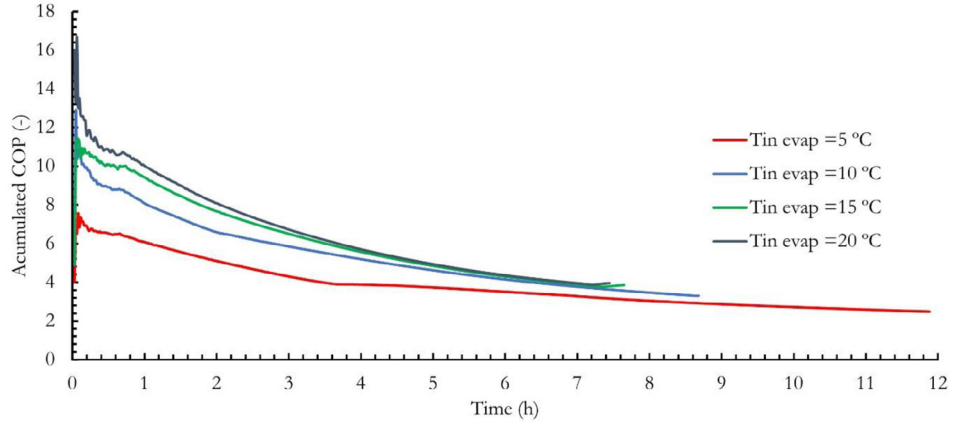

c)

Fig. 5. (a) Temperature T_1 evolution with time during the heating process as a function of the evaporator inlet temperature. (b) Instantaneous COP evolution with time. (c) Accumulated COP evolution with time.

as in the present study. In case the thermal losses in the pipes were important they should be taken into account in order to correct the actual temperature difference in Equation 13 by considering:

$$(T_{top} - T_{bottom}) \approx \frac{\dot{Q}}{\dot{m} \cdot C_p} + \Delta T_{losses} = \frac{\dot{W} \cdot COP}{\dot{m} \cdot C_p} + \Delta T_{losses} \quad (14)$$

In light of Equation 13, the potential evolution of averaged Ri with mass flow rate is similar to that found in Fig. 4 for the global COP, and it permits explaining the evolution of global COP found in Fig. 4. As shown in Fig. 4, at high flow rates (0.25 and 0.305 kg·s^{-1}) the time-averaged COP of the CO_2 heat pump follows a decreasing trend whereas the global COP of the system does not decrease at high flow rates but, on the contrary, it settles, following a similar

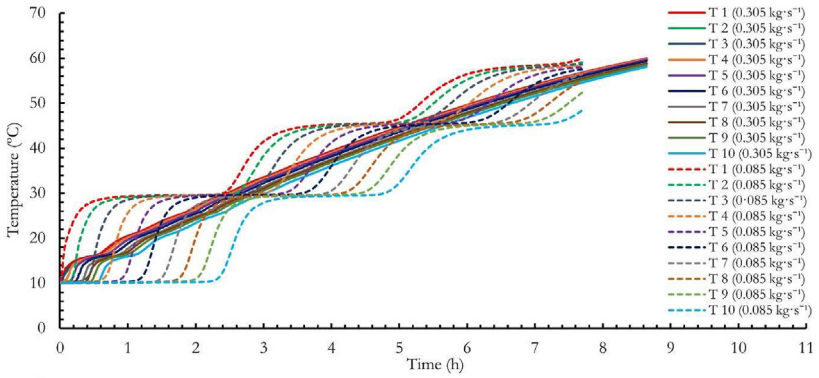

a)

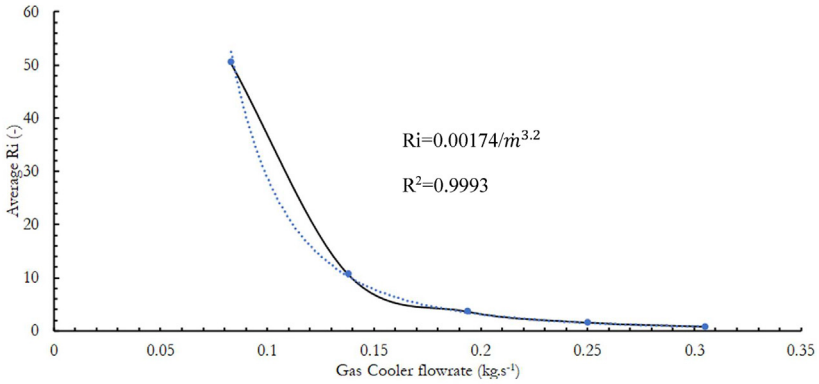

b)

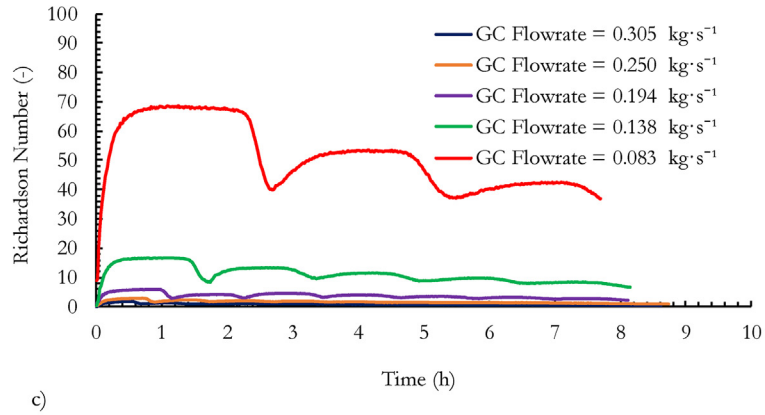

c)

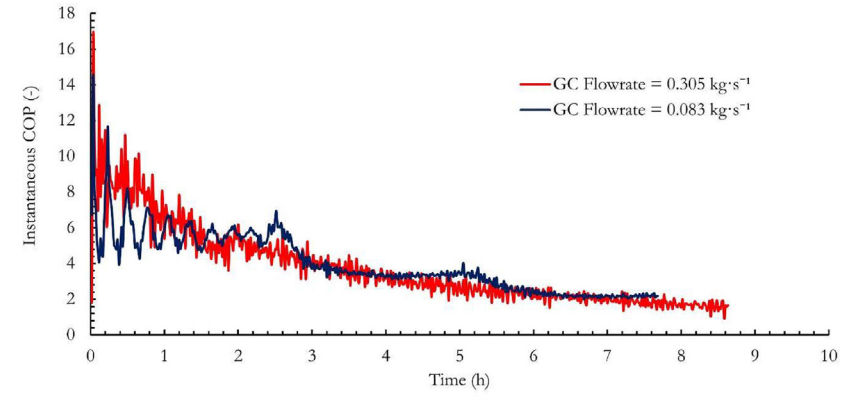

d)

Fig. 6. (a) Comparison of temperature evolution at different heights of the hot water storage tank for the case of low and high water mass flow rate at the gas cooler. (b) Maximum Ri vs mass flow rate. (c) Evolution of Ri during the storage tank heating process for different mass flow rates. (d) Evolution of the instantaneous COP during the heating process for low and high mass flow rates at the gas cooler.

tendency of the Ri number of Fig. 6b. As can be inferred from the definition equations of both COPs, this difference in the evolution of both COPs is mainly related to the hot water storage tank regime during the heating process and its stratification. Regarding the time evolution (Fig. 6c), Ri increases from zero to a maximum value, during the heating process of the water of the tank. It is also worth noting that the oscillations in the Ri evolution for low mass flow rates have a period of the order of $\sim t_c$ and coincide with the time location of the temperature steps (Fig. 6c) which have an amplitude proportional to these temperature steps, i.e. $\propto \frac{\dot{Q}}{\dot{m}\cdot C_p}$. At the end of the heating period, the stratification found with the lowest flow rate is 40 times higher than that found for the highest flow rate. Fig. 6c shows that Ri $\sim$ 40 in the system is enough to ensure tank stratification whereas Ri $\sim$1 (i.e. vertical filling velocities at the tank $v \sim \frac{4\dot{m}}{\rho\pi D^2}$ of the order of $\sim$0.5–0.6 mm·s^{-1} in tests 4 and 5) inhibit stratification and promote mixing. For the case of a water flow rate of 0.138 kg·s^{-1}, which corresponds to Ri $\sim$10 the stratification is deficient (with a temperature gradient of $\sim$ 4 K/m), whereas for the case of 0.083 kg·s^{-1} i.e. Ri $\sim$ 40 the stratification is better stablished (with a temperature gradient of $\sim$ 8 K/m). It is worth remarking that there is not a clear threshold line but a fuzzy band that defines the transition regime between stratified and non-stratified conditions. The region between Ri $\in$ [10,40] could be considered as a transition region where the flow regime evolves towards a stable, stratified regime. Under this perspective, the value of Ri $\sim$ 40 should be understood as a minimum reference order of magnitude that maintains the stratification in the storage tank. Thus, when coupling a CO_2 heat pump with a hot-water storage tank, H', d, $\dot{m}$, $\dot{W}$ and *COP* must be selected to ensure a minimum order of magnitude of Ri $\sim$ 40. Note that, during the estimation of the order of magnitude of the Ri in the design process of a DHW system, $\dot{W}$and *COP* can be obtained from the reference values provided by the manufacturer of the heat pump. Once selected the tank and the heat pump, the gas cooler mass flow rate is the variable that can be changed by the control system and/or the user in order to promote stratification and improve the global COP of the system.

A low flow rate in the gas cooler not only has a great benefit in the thermal stratification but also on the thermal performance of the system. From Fig. 6a can be seen that the temperature of the bottom of the tank in the case of the low flow rate is always lower than that of the higher flow rate. This results in a low inlet temperature to the gas cooler which enhances the efficiency of the heat pump and the whole system. Fig. 6d presents the evolution of the instantaneous COP of the DHW production system as a function of time for both tests. It can be seen that the COP is relatively high in the first third of the heating process and then it decreases with the increase of time for both tests conditions. In the case of a high flow rate in the gas cooler, the instantaneous COP is higher in the first hour than that of the case with low flow rate and then it equals or it is slightly below it. Note that in this last case, the instantaneous COP has three time steps of the order of $\sim t_c$ which are related to the temperature steps noticed at the bottom of the hot water storage tank due to the tank stratification. Besides, in this case, the instantaneous COP also shows some oscillations within the first 2.5 h (i.e. first time step). This is a general pattern shown at low flow rates. The lower the flow rate, the sharper the oscillations. These are due to the water temperature heating "jumps" found at different heights within the tank (Fig. 3d) and have its characteristic time which of the order of $\sim H/(10v) \sim \frac{H\rho\pi D^2}{40\dot{m}}$. As shown in Equation 2, these temperature heating "jumps" at the different water layers of a stratified tank are included on the numerator of the instantaneous COP equation. Consequently, the oscillations presented in Fig. 6d at a low flow rate corresponds to the curve shape resulting from the sum of the curves shown in Fig. 3d. All in all, as shown in Table 6, the global COP of the system is better in the case of low flow rates than in the case of high flow rates. This variation in the global COP reaches 12.4% when comparing the global COP at the lowest flow rate (test 1) which is 3.688 with the one at the highest flow rate (test 5). In part, this variation is due to the shorter tank heating time of the low flow rate case.

Results showed that, when heating the water storage tank with CO_2 water-to-water heat pumps, strategies based on promoting stratification, such as the use of the minimum possible water flow rate between the tank and the heat pump gas cooler, permits to reduce around 16% the electric power consumption of the compressor during the heating compared to other strategies. However, strategies based on considering higher water flow rates in the gas cooler enhances the water mixing, increase the heating time needed to reach T_{hwr} temperature at the top of the storage tank and reduce the global COP of the systems.

In the case of the present study, the difference between the use of low or high mass flow rate strategies (test 1 vs test 5) results in an increase of 19% of energy consumption at the compressor during the heating process and a variation of 25% in the global COP of the system of the last third of the heating period (Table 6). As a result, the operating strategy that maximizes the global COP of the system depends on the specific DHW consumption profile. For the case of small and/or time spaced DHW consumption profiles, the use of low flow rates is recommended as they ensure the maintenance of the stratification and shorter heating periods (and therefore energy consumption) to reach the T_{hwr}. However, in cases where high and/or intensive DHW consumption profiles are expected, a strategy based on whether increasing the T_{hwr} keeping a low mass flow rate or using high gas cooler water flow rates might be interesting as this strategy provides higher stored thermal energy.

4.5. Comparison of the present results with similar experimental studies

As previously discussed in the introduction section, there are very few experimental works devoted to the analysis of the overall performance of CO_2 heat pumps coupled with a storage tank in a whole DHW production system. One of the few authors that performed experimental tests in a CO_2 heat pump water heater similar to the one tested in this work are Tosato et al. [32]. The comparison of those results with the present work is presented in Table 8. In their work, Tosato et al. reported COP values that ranged from 5.1 in the first period, when the temperature of the water entering the gas cooler reached $T_{gcin} \approx 20°C$, to an average COP of 4.0 for the whole test, which finished when $T_{ingc} = 32°C$, As those tests were performed with an evaporator inlet temperature $T_{inevap} \approx 15°C$, they can be compared to our test number 8, which yields an accumulated COP of 9.7 for the first 80 min, when $T_{ingc} \approx 20°C$, and an accumulated COP of 7.47 for the first 180 min, when $T_{ingc} \approx 32°C$. Those important differences can be explained by the differences in the pressure control strategy. Tosato's tests were performed operating the CO_2 heat pump with a constant gas cooler pressure around 105 bar, which means that the system operated following a transcritical cycle. On the contrary, as will be explained in detail in section 4.6, all our tests were performed with a variable (optimal) gas cooler pressure control, that maintains the system operating under subcritical conditions until $T_{ingc} \approx 30°C$ and clearly improves the system's efficiency.

Other authors that present results obtained in a CO_2 heat pump water heater similar to ours are Liu et al. [33], although during their tests the water temperature continuously changed in both,

Table 8
Summary of the comparison of the present results with previous works.

Instantaneous COP						Accumulated COP			
Liu's work			Present work			$T_{in\ evap}$ (°C)	$T_{in\ gc}$ (°C)	COP	
$T_{in\ evap}$ (°C)	$T_{in\ gc}$ (°C)	COP	$T_{in\ evap}$ (°C)	$T_{in\ gc}$ (°C)	COP			Tosato's work	Present work
27	27	3.65	20	27	6	15	10 → 20	5.1	9.7
27	35	3.05	20	35	4.53				
16	43.5	2.5	16	43.5	3.6	15	10 → 32	4	7.47
10	53.3	2.1	10	53.3	2.6				

the evaporator inlet and the gas cooler inlet, which makes them even more difficult to compare with our results. They provide instantaneous COP values for different compressor frequency (f), hot water flow rate (V_h), cold water flow rate (V_c), or expansion valve opening (n) during the whole heating process, that started with both tanks at 27 °C and finished when the hot tank reached 60 °C. Table 8 compares Liu's instantaneous heating COP for f = 50 Hz, V_h = 0.4 $m^3 \cdot h^{-1}$, V_c = 0.2 $m^3 \cdot h^{-1}$ and n = 330, with those obtained under similar operating conditions in our facility. For this particular case, Liu's instantaneous heating COP varied from COP = 3.65 at the beginning of the process, when the systems had been operated for t = 1000 s (i.e., $T_{ingc} = T_{inevap} = 27$ °C), to COP = 3.05 when the systems had been operated for t = 1000 s (i.e., $T_{in\,gc} \approx 35°C, T_{in\,evap} \approx 27°C$), COP = 2.5 for t = 4000 s ($T_{in\,gc} \approx 43.5°C, T_{in\,evap} \approx 16°C$), and COP = 2.1 towards the end of the heating process (i.e., t = 6000 s, $T_{in\,gc} \approx 53.3°C, T_{in\,evap} \approx 10°C$). In our case, for similar conditions we obtained better COP values (6, 4.53, 3.6, and 2.6 for the corresponding equivalent conditions). Although those differences could be explained by differences in the gas cooler pressure control strategy, Liu does not provide clear information about this point and, therefore, no definitive conclusions can be drawn.

4.6. Influence of the operation mode of the CO_2 heat pump on the COP of the DHW generation system: transcritical vs subcritical cycle

In the case of the CO_2 heat pump used in the present study, the back-pressure electronic valve seeks for the optimal gas cooler pressure in the refrigerant side in order to maximise the COP of the heat pump. This control strategy permits the heat pump to work with a gas cooler pressure over or under the critical pressure of the CO_2. As indicated in the test methodology section, during the tests it was logged the evolution of the working pressure of the refrigerant at the gas cooler with time, in order to evaluate whether the CO_2 heat pump was working with a transcritical or a subcritical thermodynamic cycle.

Fig. 7 shows the T-s working diagrams of the CO_2 heat pump for the case of test 1 and 5. These tests have a water mass flow rate at the gas cooler of 0.083 $kg \cdot s^{-1}$ and 0.305 $kg \cdot s^{-1}$, respectively. In both cases it is shown two representative examples of the working cycle: one at the beginning of the heating test and another at the end of the heating test. In order to properly compare the operation mode of the heat pump, the cases selected for test 5 have a similar water temperature at the gas cooler inlet to that of the test 1. In the figure, the black line represents the thermodynamic states of the refrigerant (i.e. CO_2) and the blue line represents thermodynamic states of the water at the gas cooler during the heating process. The figure also shows the instantaneous COP of the heat pump for the lapse of time shown in the T-s cycle. As shown, during the beginning of the heating process (left side of the figure), the water temperature at the inlet of the gas cooler is relatively low and the heat pump works under a subcritical mode with a gas cooler optimal pressure at the refrigerant side below the critical pressure of the CO_2. In this case there is a phase change of the CO_2 and the gas cooler works as a condenser. This subcritical operational mode at the beginning of the heating process is found for all the water mass flow rate conditions tested. It is also found that the higher the mass flow rate, the lower gas cooler optimal pressure stablished: In the case of 0.083 $kg \cdot s^{-1}$, it is reached 60 bars, whereas the case of 0.305 $kg \cdot s^{-1}$ it is reached 52 bars. This operational mode results in a lower pressure ratio and a lower power consumption at the compressor. As a consequence, there is a "boost" of the instantaneous COP of the heat pump compared to the case of transcritical operation mode when COP reported are between 2 and 3 times lower. Besides, the higher mass flow rate at the gas cooler of test 5 provides a lower gas cooler working pressure and an increase of 50% in the instantaneous heat pump COP when compared with test 1. This explains the lower average COP of the DHW production system in the first third of the heating period reported in Table 6 for test 1 with respect to that of test 5. Thus, in the case of the heat pump working under a subcritical operation mode it is recommended to set high water mass flow rates in order to maximize the COP of the DHW production system.

During the end of the heating process (right side of the figure), the water temperature at the inlet of the gas cooler is higher and the heat pump works under a transcritical mode with a gas cooler pressure at the refrigerant side over the critical pressure of the CO_2. In this case the optimal working pressure at the gas cooler is much higher (around 105 bars) and the instantaneous COP of the heat pump is drastically reduced when compared to the subcritical operation mode. Moreover, the difference of the gas cooler working pressure between test 1 and 5 is considerably reduced to less than 0.7 bars (it is 105.6 bars in the case of 0.083 $kg \cdot s^{-1}$, and 105.0 bars in the case of 0.305 $kg \cdot s^{-1}$). This shows that the influence of the water mass flow rate at the gas cooler strongly influences the COP of the heat pump when it works under a subcritical cycle (i.e. with low inlet water temperatures at the gas cooler) whereas this influence of the water mass flow rate almost vanishes when the inlet temperature of the water at the gas cooler is relatively high and the heat pump works under a transcritical cycle.

All in all, it is found that in order to maximize the COP of the DHW production system, the heat pump should work with high mass flow rates when it operates under subcritical mode (i.e. at the beginning of the tank heating process when the water temperature at the bottom of the tank is low) and it should "switch" to low mass flow rates when it works under a transcricical operation mode (i.e. during the rest of the tank heating process, when the water temperature at the bottom of the tank is higher). This change in the mass flow rate should be progressive as the heat pump evolves from subcritical towards transcritical operation modes always seeking the maximization of COP of the DHW production system.

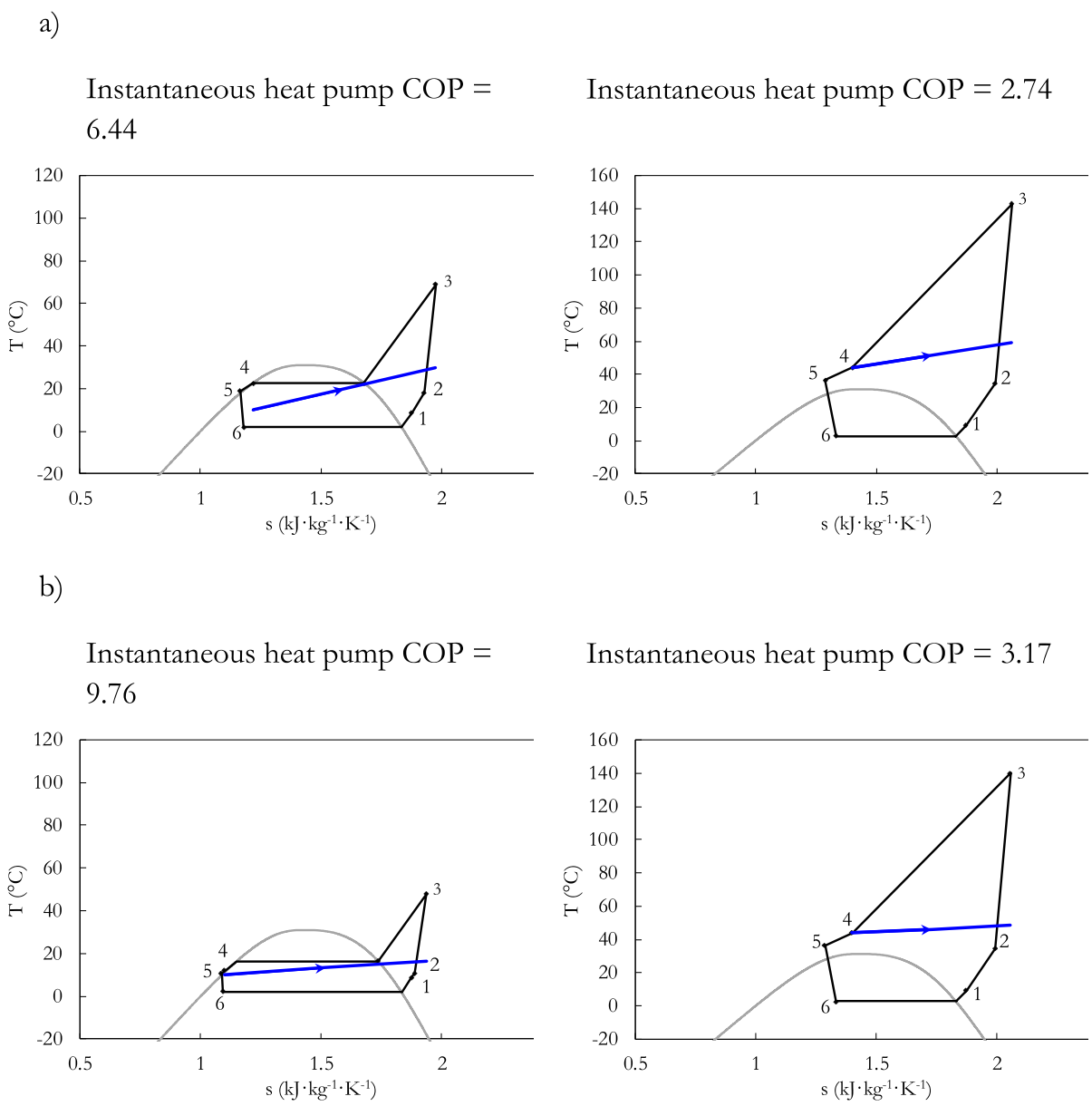

Fig. 7. Operation mode of the heat pump: T-s cycles of the CO_2 heat pump working at the beginning of the heating process (left) and at the end of the heating process (right). (a) test 1: gas cooler water mass flow rate 0.083 kg·s^{-1}. (b) test 5: gas cooler water mass flow rate 0.305 kg·s^{-1}.

5. Conclusions and future work

This work has focused on the experimental characterization of the dynamic performance of a DHW production system working with CO_2 water-to-water heat pump connected to a hot-water storage tank. By developing an ad-hoc experimental facility, the results of the tests showed that the water control strategy is a key factor in the overall performance of the DHW production system:

- In the case of minimum water flow rate at the gas cooler, results showed that the overall performance of the DHW system increased compared to the case of other flow rates, as the filling process does not induce the mixing of water what promotes that the upper layer of the tank, where the DHW for consumption is obtained, always maintains the highest temperature of the tank. Moreover, the stratification also reduces the heating time. However, very low flow rates also reduce the overall thermal energy stored in the tank. Therefore, there must be a compromise between energy efficiency and capacity to supply the thermal energy demanded by the user.
- Stratification is a key factor in the energy efficiency of the system. Considering a heating strategy where stratification is maintained by establishing the minimum water flow rate at the gas cooler (test 1), the electric consumption of the compressor can be reduced by 25% compared to the case of setting the maximum was flow rate at the gas cooler (test 5).
- Reaching tank Ri numbers $\sim$ 40 during the heating process (i.e. vertical filling velocities at the hot-water storage tank $v \sim 0.1$ mm·s^{-1}) ensures stratification whereas Ri $\sim$ 1 (i.e. velocities $v \sim 0.5$–0.6 mm·s^{-1}) inhibit stratification and promotes mixing. This means that a reduction of a factor of 3.7 in the mass flow rate results in an increase of the stratification in a factor of 40. Thus, when coupling a CO_2 heat pump with a hot-water storage tank, H', d, $\dot{m}$, W *and COP* must be selected to ensure

a minimum order of magnitude of $Ri \approx \frac{\pi^2 d^4 g \cdot H' \cdot \rho^2 \cdot \beta \cdot \dot{W} \cdot COP}{16 \cdot C_p \cdot m^3} \sim 40$.

- The use of a heating strategy based on setting high water flow rates at the gas cooler enhances the water mixing, which reduces the global COP of the DHW production system due to three factors: the reduction of the water temperature at the top of the storage tank, the reduction of the COP of the CO_2 heat pump due to the increase of the water temperature at the inlet of the gas cooler and the increase of the heating time and the compressor working time needed to reach the set point temperature at the top of the storage tank. Besides, a reduction in the gas cooler mass flow rate of ~ 72% results in a reduction of ~ 6% in the overall thermal energy stored in the tank which means a $dE_{tank}/d\dot{m} \approx 41$ kJ·Kg^{-1}·s^{-1}).
- The increase of the evaporator inlet water temperature from 5 °C to 20 °C increases the global COP of the DHW production system by 59% during the heating process which means a reduction of ~ 3.9% per degree increased at the inlet evaporator water temperature. Besides, it also reduces the heating time by around ~ 40% which means a reduction of the heating time of around 2.7% per degree increased at the inlet evaporator water temperature ($dt_{tank}/dT_{in\ evap} \sim 1/3$ (h/°C)).
- In order to maximize the COP of the DHW production system, the heat pump should work with high mass flow rates when it operates under subcritical mode (i.e. at the beginning of the tank heating process when the water temperature at the bottom of the tank low) and it should "switch" to low mass flow rates when it works under a transcricical operation mode (i.e. during the rest the tank heating process when the water temperature at the bottom of the tank is higher).

The methodology followed in the study can be used to assist in the design and dynamic characterization of the behaviour of CO_2 water-to-water heat pumps for DHW production systems. Future work will focus on the development of a numerical model of the hot water storage tank and the use of this experimental data to validate numerical simulations obtained with the numerical model to predict the system behaviour during other stages of the operation of the DHW production system under standard conditions.

Declaration of Competing Interest

The authors declare that they have no known competing financial interests or personal relationships that could have appeared to influence the work reported in this paper.

Acknowledgements

This work has been performed in the context of the project in the project "Maximisation of the efficiency and minimisation of the environmental impact of heap pumps for the decarbonisation of heating and domestic hot water production in nearly zero energy buildings" ENE2017- 83665-C2-2-P, Funded by the Ministry of Economy and Competitiveness, Spain and the support of the European Regional Development Fund.

References

[1] Communication from the commission to the European parliament, the European council, the council, the European economic and social committee and the committee of the regions The European Green Deal, COM/2019/640 final.
[2] A. Allouhi, Y. El Fouih, T. Kousksou, A. Jamil, Y. Zeraouli, Y. Mourad, Energy consumption and efficiency in buildings: current status and future trends, J. Clean Prod. 109 (2015) 118–130, https://doi.org/10.1016/j.jclepro.2015.05.139.
[3] Eurostat. Energy consumption in households by type of end-use, 2018. https://ec.europa.eu/eurostat/statistics-explained/index.php?title=Energy_consumption_in_households.
[4] A. Bastani, P. Eslami-Nejad, M. Badache, A.T.A. Nguyen, Experimental characterization of a transcritical CO2 direct expansion ground source heat pump for heating applications, Energy Build. 212 (2020) 109828, https://doi.org/10.1016/j.enbuild.2020.109828.
[5] C. Mateu-Royo, C. Arpagaus, A. Mota-Babiloni, J. Navarro-Esbrí, S.S. Bertsch, Advanced high temperature heat pump configurations using low GWP refrigerants for industrial waste heat recovery: a comprehensive study, Energy Convers Manag. 229 (2021) 113752, https://doi.org/10.1016/j.enconman.2020.113752.
[6] K.J. Chua, S.K. Chou, W.M. Yang, Advances in heat pump systems: A review, Appl. Energy 87 (12) (2010) 3611–3624, https://doi.org/10.1016/j.apenergy.2010.06.014.
[7] H. Esen, M. Inalli, M. Esen, K. Pihtili, Energy and exergy analysis of a ground-coupled heat pump system with two horizontal ground heat exchangers, Build. Environ. 42 (2007) 3606–3615, https://doi.org/10.1016/j.buildenv.2006.10.014.
[8] M.a. Liangdong, R. Tixiu, Z. Tianjiao, Z. Tianyi, Z. Jili, Experimental study on effect of operating parameters on performance of serially cascaded wastewater source heat pump, J. Build. Eng. 32 (2020) 101458, https://doi.org/10.1016/j.jobe.2020.101458.
[9] P. Farzanehkhameneh, M. Soltani, F. Moradi Kashkooli, M. Ziabasharhagh, Optimization and energy-economic assessment of a geothermal heat pump system, Renew. Sustain. Energy Rev. 133 (2020) 110282, https://doi.org/10.1016/j.rser.2020.110282.
[10] O. Bamigbetan, T.M. Eikevik, P. Nekså, M. Bantle, Review of vapour compression heat pumps for high temperature heating using natural working fluids, Internat. J. Refrig. 80 (2017) 197–211, https://doi.org/10.1016/j.ijrefrig.2017.04.021.
[11] F. Illán-Gómez, V.F. Sena-Cuevas, J.R. García-Cascales, F.J.S. Velasco, Experimental and numerical study of a CO2 water-to-water heat pump for hot water generation, Int. J. Refrig 132 (2021) 30–44, https://doi.org/10.1016/j.ijrefrig.2021.09.020.
[12] F. Illán-Gómez, V.F. Sena-Cuevas, J.R. García-Cascales, F.J.S. Velasco, Analysis of the optimal gas cooler pressure of a CO2 heat pump with gas bypass for hot water generation, Appl. Therm. Eng. 182 (2021) 116110, https://doi.org/10.1016/j.applthermaleng.2020.116110.
[13] Y. Song, F. Cao, The evaluation of optimal discharge pressure in a water-precooler-based transcritical CO2 heat pump system, App Therm Eng. 131 (2018) 8–18, https://doi.org/10.1016/j.applthermaleng.2017.11.092.
[14] E. Brodal, S. Jackson, A comparative study of CO2 heat pump performance for combined space and hot water heating, Internat. J. Refrig. 108 (2019) 234–245, https://doi.org/10.1016/j.ijrefrig.2019.08.019.
[15] J.-H. Cheng, Y.-J. He, C.-L. Zhang, New scenario of CO2 heat pump for space heating: Automatic mode switch between modified transcritical and cascade cycle in one system, Appl. Therm. Eng. 191 (2021) 116864, https://doi.org/10.1016/j.applthermaleng.2021.116864.
[16] B. Dai, H. Qi, W. Dou, S. Liu, S. Zhong, H. Yang, V. Nian, Y. Hao, Life cycle energy, emissions and cost evaluation of CO2 air source heat pump system to replace traditional heating methods for residential heating in China: System configurations, Energy Conver. Manage. 218 (2020) 112954, https://doi.org/10.1016/j.enconman.2020.112954.
[17] Z. Wang, F. Wang, Z. Ma, W. Lin, H. Ren, Investigation on the feasibility and performance of transcritical CO2 heat pump integrated with thermal energy storage for space heating, Renewable Energy 134 (2019) 496–508, https://doi.org/10.1016/j.renene.2018.11.035.
[18] Z. Wang, Y. Zheng, F. Wang, M. Song, Z, Ma Study on performance evaluation of CO2 heat pump system integrated with thermal energy, storage for space heating, Energy Procedia 158 (2019) 1380–1387, https://doi.org/10.1016/j.egypro.2019.01.338.
[19] Nicholas Fernandez, Yunho Hwang, Reinhard Radermacher, Comparison of CO2 heat pump water heater performance with baseline cycle and two high COP cycles, Int. J. Refrig 33 (3) (2010) 635–644, https://doi.org/10.1016/j.ijrefrig.2009.12.008.
[20] Sung Goo Kim, Yoon Jo Kim, Gilbong Lee, Min Soo Kim, The performance of a transcritical CO2 cycle with an internal heat exchanger for hot water heating, Int. J. Refrig 28 (7) (2005) 1064–1072, https://doi.org/10.1016/j.ijrefrig.2005.03.004.
[21] Ryohei Yokoyama, Tetsuya Wakui, Junya Kamakari, Kazuhisa Takemura, Performance analysis of a CO2 heat pump water heating system under a daily change in a standardized demand, Energy 35 (2) (2010) 718–728, https://doi.org/10.1016/j.energy.2009.11.008.
[22] Bin Hu, Xiaolin Wang, Feng Cao, Zhilong He, Ziwen Xing, Experimental analysis of an air-source transcritical CO2 heat pump water heater using the hot gas bypass defrosting method, Appl. Therm. Eng. 71 (1) (2014) 528–535, https://doi.org/10.1016/j.applthermaleng.2014.07.017.
[23] I.J. Moncho-Esteve, M. Gasque, P. González-Altozano, G. Palau-Salvador, Simple inlet devices and their influence on thermal stratification in a hot water storage tank, Energy Build. 150 (2017) 625–638, https://doi.org/10.1016/j.enbuild.2017.06.012.
[24] Zilong Wang, Hua Zhang, Binlin Dou, Huajie Huang, Weidong Wu, Zhiyun Wang, Experimental and numerical research of thermal stratification with a novel inlet in a dynamic hot water storage tank, Renewable Energy 111 111 (2017) 353–371, https://doi.org/10.1016/j.renene.2017.04.007.

[25] L. Gao, H. Lu, B. Sun, D. Che, L. Dong, Numerical and experimental investigation on thermal statificacion characteristics affected by the baffle plate in the thermal storage tank, J. Energy Storage (2021), https://doi.org/10.1016/j.est.2020.102117 102117.
[26] Z. Wang, H. Zhang, H. Huang, B. Dou, X. Huang, M.A. Goula, The experimental investigation of the thermal stratification in a solar hot water tank, Renewable Energy 134 (2019) 862–874, https://doi.org/10.1016/j.renene.2018.11.088.
[27] M. Esen, T. Ayhan, development of a model compatible with solar assisted cylindrical energy storage tank and variation of stored energy with time for different phase change materials, Energy Convers. Mgmt 37 (1996) 1775–1785.
[28] Y.P. Chandra, T. Matuska, Numerical prediction of the stratification performance in domestic hot water storage tanks, Renewable Energy 154 (2020) 1165–1179, https://doi.org/10.1016/j.renene.2020.03.090.
[29] Jørn Stene, Residential CO2 heat pump system for combined space heating and hot water heating, Int. J. Refrig 28 (8) (2005) 1259–1265, https://doi.org/10.1016/j.ijrefrig.2005.07.006.
[30] Jørn Stene, Residential CO2 heat pump system for combined space heating and hot water heating. PhD Thesis.
[31] G. Tosato, P. Artuso, S. Minetto, A. Rossetti, Y. Allouche, K. Banasiak, Experimental and numerical investigation of a transcritical CO2 air/water reversible heat pump: analysis of domestic hot water production. 14th Gustav Lorentzen Conference, Kyoto, Japan, 6th- 9th December 2020.
[32] G. Tosato, S. Girotto, S. Minetto, A. Rossetti, S. Marinetti, An integrated CO2 unit for heating, cooling and DHW installed in a hotel. Data from the field. 37th UIT Heat Transfer Conference. 2019. doi:10.1088/1742-6596/1599/1/012058.
[33] F. Liu, W. Zhu, Y. Cai, E.A. Groll, J. Re, Y. Lei, Experimental performance study on a dual-mode CO2 heat pump system with thermal storage, Appl. Therm. Eng. 115 (2017) 393–405, https://doi.org/10.1016/j.applthermaleng.2016.12.095.
[34] I. Sifnaiosa, J. Fana, L. Olsenb, C. Madsenb, S. Furboa, Optimization of the coefficient of performance of a heat pump with an integrated storage tank, Appl. Therm. Eng. 160 (2019), https://doi.org/10.1016/j.applthermaleng.2019.114014 114014.
[35] F. Aguilar, D. Crespí-Llorens, S. Aledo, P.V. Quiles, One-dimensional model of a compact DHW heat pump with experimental validation, Energies 14 (2021) 2991, https://doi.org/10.3390/en14112991.
[36] European Committee for Standardization (ECS), EN 16147, heat pump with electrically driven compressor testing, performance rating and requirements for making of domestic hot water units. Spanish standard UNE- EN 16147. December 2017.
[37] W. Li, P. Hrnjak, Experimentally validated model of heat pump water heater with a water tank in heating-up transients, Int. J. Refrig 88 (2018) 420–431, https://doi.org/10.1016/j.ijrefrig.2018.01.020.
[38] National Instruments, Ni-Data Acquisition Ni-DAQ Specifications cDAQ™-9189, 2017.
[39] Agilent Technologies, Agilent Datalogger. Agilent 34970A/34972A Data Acquisition / User's Guide, 2012.
[40] I.S.O. Standard, Guide for Uncertainty Estimation In Measurements, International Standardisation Organization, Switzerland, 1999.
[41] A. Karim, A. Burnett, S. Fawzia, Investigation of stratified thermal storage tank performance for heating and cooling applications, Energies 11 (2018) 1049, https://doi.org/10.3390/en11051049.
[42] Joseph Rendall, Ahmad Abu-Heiba, Kyle Gluesenkamp, Kashif Nawaz, William Worek, Ahmed Elatar, Nondimensional convection numbers modeling thermally stratified storage tanks: Richardson's number and hot-water tanks, Renew. Sustain. Energy Rev. 150 (2021) 111471, https://doi.org/10.1016/j.rser.2021.111471.